Chapter 1

Magnetic-Graphene-Based Nanocomposites and Respective Applications

Oxana Vasilievna Kharissova, Beatriz Ortega García, Boris Ildusovich Kharisov and Ubaldo Ortiz Méndez

Additional information is available at the end of the chapter

http://dx.doi.org/10.5772/64319

Abstract

Preparation, properties, and applications of magnetic-graphene-based nanocomposites are reviewed. Graphene magnetic nanocomposites include those on the basis of elemental metals (Fe, Co, Ni), magnetic nanoclusters, various morphological forms of iron oxides (Fe_2O_3, Fe_3O_4), ferrites MFe_2O_4, 3D graphene aerogels@hierarchical Fe_3O_4 nanoclusters, single-molecule magnets like $TbPc_2$ (Pc: phthalocyanine), other organometallic-containing composites (benzene-metal-graphene), as well as polycomponent nanocomposites such as $Ag/Fe_3O_4/G$ (G: graphene), $Fe_3O_4/CdS/G$, or $FePc/Fe_3O_4/GO$ (GO: graphene oxide), among others. Their available synthesis methods consist commonly of hydrothermal and solvothermal techniques, sol-gel autocombustion, sonoelectrochemical polymerization, thermal expansion and thermal reduction, microwave-assisted technique, and covalent bonding chemical methods. Their current and potential applications are distinct devices, in particular for colorimetric detection of glucose, construction materials, analytical, sensor and biosensor applications, environmental remediation, compounds with antibacterial properties, catalysis and photocatalysis, biological imaging, oil absorption, etc.

Keywords: environmental applications, ferrites, grapheme, hybrids, iron oxides, lithium batteries, magnetic composites, metals

1. Introduction

Graphene, which consists in a single layer of carbon atoms, has been intensively studied in the last decade due to its extraordinary structural and electronic properties, leading to numerous current and potential applications in electronic devices. Growing, doping, or adsorption of metal

nanoparticles and other inorganic/organic species on its surface can change, improve, and manipulate graphene magnetic and electronic properties. If these particles possess magnetic properties, the whole nanocomposite can have them too, opening new opportunities and applications for the formed hybrids.

Currently, the information on magnetic graphene and graphene oxide nanocomposites has not yet been extensively reviewed despite a number of original reports. At the same time, their importance is undoubtful due to numerous current and potential applications of graphene itself, and magnetic nanoparticles in a variety of fields of chemistry, physics, medicine and biology, in the frontiers with nanotechnology. This topic is rarely presented as short sections in some reviews [1–4], dedicated to graphene, in contrast to carbon nanotubes, where a concise review was recently published [5]. So, the main purpose of this chapter is to highlight magnetic graphene composites, and review their main synthesis methods, properties, and current and potential applications.

2. Metal-graphene composites

A certain number of magnetic metals are present in the Periodic Table. Graphene composites have been reported only with some typical metals with paramagnetic properties, such as iron, cobalt, or nickel. Among theoretical studies of metal interactions with graphene surface, quantum Monte Carlo methods, studying the consequences of placing a magnetic adatom adjacent to a vacancy in a graphene sheet [6, 7], and description of electronic and magnetic properties of the graphene-ferromagnet interfaces [8] are particularly relevant. In addition, the plane-wave density functional theory (DFT) was used to study the properties of nanostructures of the type C_{60}-M-G (M: Ti, Cr, Mn, Fe, or Ni; G: graphene) [9]. In this work, in particular, it was found that the high-spin C_{60}-Cr-G nanostructure is more stable than its low spin analog. Structures containing distinct metals can be different. For instance, on the graphene surface, C_{60}-Ti stands symmetrically upright, while for other metals, C_{60}-M fragments are bent and nonequal in each composite (**Figure 1**). Authors suggested, based on calculations, that the C_{60}-M fragment is flexible, respecting the bending motion. Importantly, the attachment of C_{60} to an M-G surface is more energetically favored than the decoration of graphene with C_{60}-metal complexes. DFT studies were also carried out for Co-G composites (cobalt-vacancy defect [10] or single Co atom incorporated with divacancy in armchair graphene nanoribbon [11]). In this case, metal dopation was found to introduce magnetic properties into the formed composite.

Several reports were dedicated to *cobalt-graphene* nanocomposites. Studying single Co atoms on graphene on Pt(111) and their magnetic properties by scanning tunneling microscopy spin-excitation spectroscopy, upon hydrogen adsorption, three differently hydrogenated species were identified (**Figure 2**) [12], whose magnetic properties are very different from those of cobalt element. It was suggested that, due to the interaction of Co-G orbitals, large magnetic anisotropy stems from strong ligand field effects that take place. A series of reports studied the *intercalation* of cobalt between graphene and Ir(111) via distinct techniques. Thus, cobalt layers intercalated in between graphene and Ir(111) were characterized by a combination of

http://dx.doi.org/10.5772/64319

X-ray magnetic circular dichroism and photoemission [13]. In particular, an induced magnetic moment in the graphene layer, antiparallelly oriented to that of cobalt, was established. Magnetic ordering was found to exist beyond monolayer intercalation. In a related report [14], cobalt-intercalated graphene on Ir(111) was studied by DFT calculations and spin-polarized scanning tunneling microscopy. It was revealed that the strong bonding between cobalt and graphene leads to a high corrugation within the Moiré pattern, which arises due to the lattice mismatch between the graphene and the Co on Ir(111).

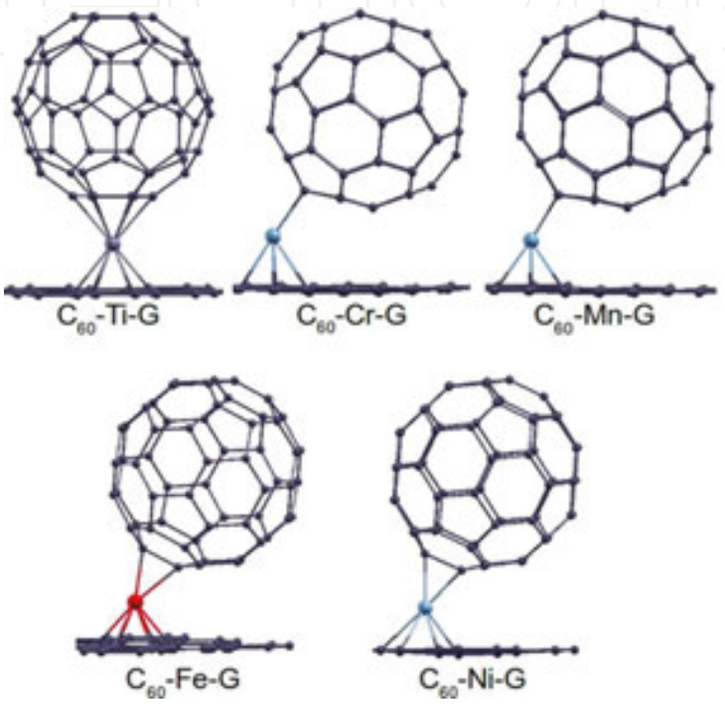

Figure 1. C_{60}-M-G nanostructures. Reproduced with permission form the *American Chemical Society*.

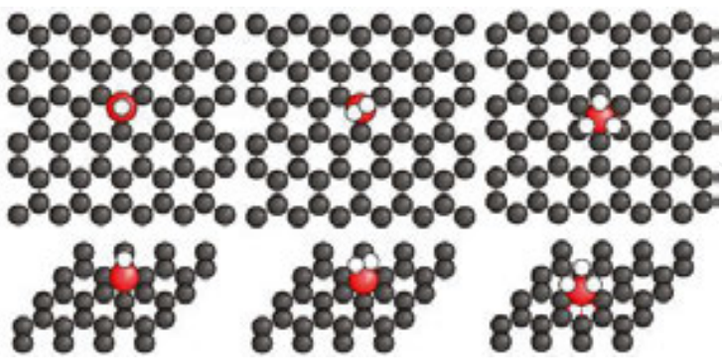

Figure 2. Top and side view of atomic structures of CoH_n (n = 1, 2, and 3) complexes. Reproduced with permission from the *APS Physics*.

In addition, nanometer-sizes films of cobalt were intercalated at the interface "graphene/Ir(111)" and were characterized by Auger electron spectroscopy and spin-polarized low-

energy electron microscopy [15]. In resulting composites, graphene top layer was found to promote perpendicular magnetic anisotropy in the Co film. It was also revealed that the magnetic anisotropy energy is significantly larger for the graphene/Co interface than for the free metallic surface. Regarding metal intercalation, contrarily to cobalt, Fe-based intercalation of GO led to the formation of reduced GO/Fe_3C magnetic hybrids [16]. Iron carbide particles were encapsulated in a graphite cage, protecting them from agglomeration.

Among other available theoretical studies on Co/G nanocomposites, the single Co layer added on graphene showed ferromagnetic ordering, with perpendicular alignment to the graphene sheet [17], according to the data obtained by relativistic density functional theory, at the level of generalized gradient approximation. These properties are promising for magnetism in 2D systems despite experimental difficulties in obtaining regular structures of single layer of this metal on graphene. In addition, the oxidation state of cobalt, together with possible oxidation of metal in real conditions, is also important. Thus, XPS spectral data for graphene/Co composites, obtained from $CoCl_2$. $6H_2O$ diluted in ethyl alcohol and highly split graphite, showed two sets of $2p_{3/2,1/2}$ lines belonging to partly oxidized and metallic Co atoms [18]. The formation of this protective oxide layer prevents metallic cobalt from deep oxidation.

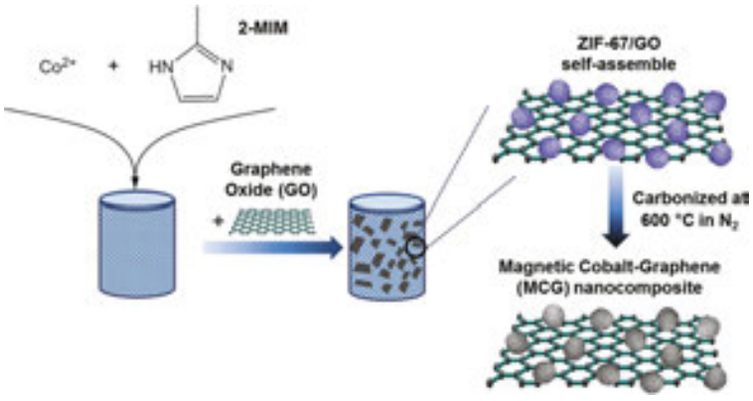

Figure 3. Scheme of synthesis of magnetic cobalt–graphene (MCG) nanocomposite. Reproduced with permission from the *Royal Society of Chemistry*.

The synthesis methods for cobalt-graphene nanocomposites frequently include high-temperature decomposition of precursors. Thus, a magnetic cobalt-G nanocomposite (**Figure 3**) was prepared by carbonizing a self-assembly of a cobalt-based metal organic framework, ZIF-67, and GO [19]. This composite based on cobalt and reduced graphene oxide (RGO) was used as a catalyst for the activation of peroxymonosulfate (PMS) in the process of decolorizing Acid Yellow dye in water. Resulting regeneration efficiency remained at 97.6% over 50 cycles, showing its effective and stable catalytic activity. The proposed mechanism of MCG activating PMS to generate sulfate radicals is shown in **Figure 4**. Another example is a combination of autocombustion and sol-gel methods, which led to Co-G nanocomposite, prepared from GO, $Co(NO_3)_2$, and citric acid as precursors [20]. A sol-gel was first prepared and then underwent autocombustion in Ar atmosphere, at 300°C, due to the action of the produced reducing agents H_2 and CH_4. In the formed nanocomposite, Co nanoparticles (with a diameter of about 10 nm)

are homogeneously distributed on graphene surface. The same technique can be applied for loading Ni, Cu, Ag, and Bi on graphene surface. Pyrolisis was also used, for instance, in the case of cobalt phthalocyanine (CoPc), for the purpose of fabricating organic metal/graphene composites [21]. CoPc is capable of dispersing cobalt and its oxide onto graphene sheets due to π-interactions between them in the conditions of pyrolysis or oxidation. The process of the fabrication of Co/GC and Co_3O_4/GC is shown in **Figure 5**. The Co_3O_4/graphene nanocomposites showed remarkable lithium storage performance, including good rate capability, good cycle performance, and highly reversible capacity. It was suggested that CuO, Fe_2O_3 and other metal or metal-oxide-based graphene composites can also be prepared in this way.

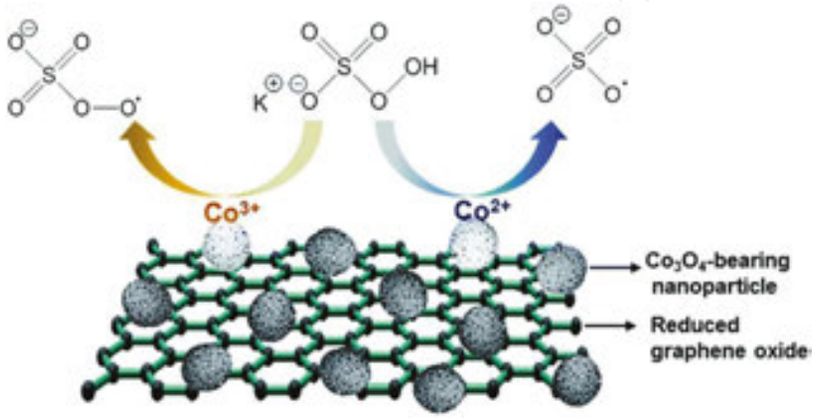

Figure 4. Proposed mechanism for PMS activation generating sulfate radicals. Reproduced with permission from the *Royal Society of Chemistry*.

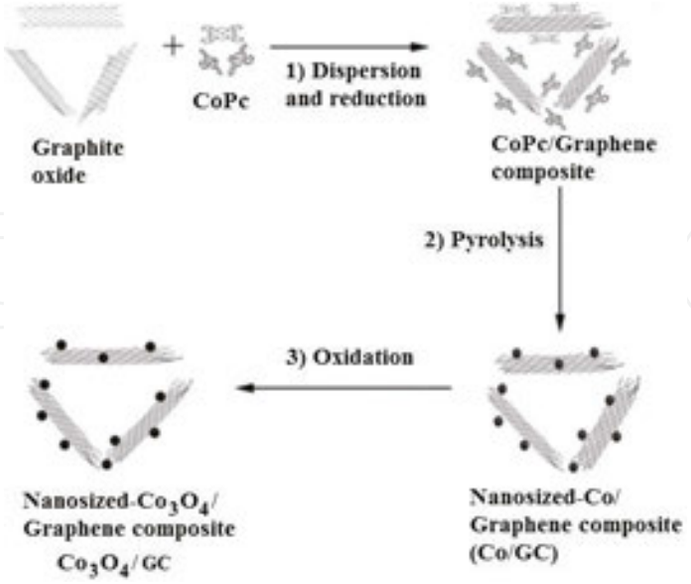

Figure 5. Fabrication of Co/GC and Co_3O_4/GC: (1) dispersion of graphite oxide and CoPc in water by ultrasonication and subsequently chemical reduction of graphite oxide, (2) pyrolysis at 800°C, and (3) oxidation at 400°C. Reproduced with permission from the *John Wiley & Sons*.

The decolorization of organic dyes, such as the Acid Yellow as mentioned above, is one of the classical applications of graphene composites of cobalt and other magnetic metals. Cobalt nanoparticles (about 30 nm size), anchored on graphene sheets, were tested for heterogeneous oxidation of a dyeing pollutant, Orange II, with peroxymonosulfate (PMS) in aqueous solutions [22]. In comparison to pure cobalt, the incorporation of Co nanoparticles into graphene sheets resulted in much higher catalytic activity for Orange II degradation. The proposed reaction mechanism is described by reactions (1)–(7). This work shows the importance of using other metal nanoparticles rather than iron for the decontamination of organic pollutants.

$Co^0 \rightarrow Co^{2+} + 2e^-$ *(1)*

$\equiv Co^0 + O_2 + 2H_2O \rightarrow \equiv Co^{2+} + 4OH^-$ *(2)*

$\equiv Co^0 + 2HSO_5^- \rightarrow \equiv Co^{2+} + 2SO_4^{-\cdot} + 2OH^-$ *(3)*

$\equiv Co^{2+} + HSO_5^- \rightarrow \equiv Co^{3+} + SO_4^{-\cdot} + OH^-$ *(4)*

$\equiv Co^{3+} + HSO_5^- \rightarrow \equiv Co^{2+} + SO_5^{-\cdot} + H^+$ *(5)*

$\equiv Co^0 + 2 \equiv Co^{3+} \rightarrow 3 \equiv Co^{2+}$ *(6)*

$SO_4^{-\cdot}$ + Orange II → many steps → $CO_2 + H_2O$ *(7)*

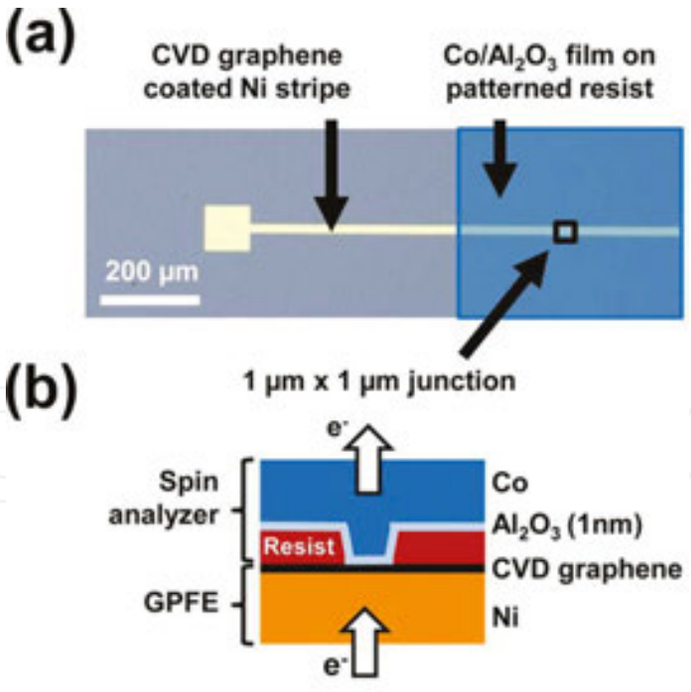

Figure 6. (a) Optical image of the device after graphene growth: an Ni stripe is coated with CVD graphene and an Al_2O_3/Co electrode is then deposited on lithographed squares in UV resist. (b) Cross-sectional scheme of the junction. Reproduced with permission from the *American Chemical Society*.

In the case of *nickel*, its graphene or GO composites are not so widespread compared to cobalt or iron. Nickel itself is used as a support for graphene fabrication, for instance, by the CVD technique of CH_4, leading to low-defect synthesis of bilayer graphene on evaporated polycrystalline nickel films [23]. The CVD method also allows to obtain nickel coated with a few layers of graphene, resulting in a stable surface upon air exposure [24]. This way, graphene-passivated (against oxidation) ferromagnetic electrodes can be fabricated, which are suitable for spin devices (namely spin-polarized oxidation-resistant electrodes as shown in **Figure 6**).

In addition to CVD, graphene or GO hybrids with nickel have also been obtained by other methods, for example, grown on a graphene Moire on Rh(111) at 150 K [25]. These processes of graphene decoration with nickel nanoparticles can include simultaneous reduction of GO in the process of synthesizing GO/Ni composites [26], in particular simultaneous reduction of GO and nickel(II) ions by the one-step far-infrared-assisted method [27]. Also, nickel nanoparticles were loaded by a graphene nanosheet by easily scalable and reproducible direct electrochemical deposition [28]. The graphene sheet decorated with magnetic nickel nanoparticles yielded a composite with soft magnetic and conductive properties, which efficiently promoted microwave absorbability (and was better than graphene alone).

Iron/graphene (or iron/GO) hybrids are very well studied and, together with other iron-containing nanostructures below (iron oxides and their combinations with iron, as $Fe@Fe_2O_3$), are undoubtedly the center of magnetic metal/graphene field. The hybrids can be obtained by several methods, both classic chemical and "greener" routes. Thus, *focused solar radiation*, as a green chemical route, was applied for the fabrication of 3D metal/metal oxide nanoparticles dispersed on 2D ultrathin graphene by a simultaneous reduction and exfoliation process [29]. This procedure allowed the insertion of nanoparticles between ultrathin graphene layers acting as "spacers" between them. These metal/metal oxide nanoparticle dispersed graphene composites might have potential applications in environmental fields, conversion devices, energy storage sensing, and heterogeneous catalysis.

Microwave irradiation was used for the synthesis (**Figure 7**) of combined hierarchical 3D graphene/carbon nanotube/iron nanostructures (G-CNT-Fe) [30]. The formed composite consists of vertically aligned CNTs, which are grown in graphene sheets along with shorter branches of CNTs stemming out from both the vertically aligned CNTs and the graphene sheets. Zero-dimensional (0D) functional iron oxide nanoparticles decorated within this 3D hierarchical nanostructure (both on 1D nanotubes and 2D graphene sheets) provide outstanding lithium storage characteristics. Iron moieties were found to be present in mixed valence states of FeOOH and Fe_2O_3. In addition, iron nanoparticles can be first deposited onto a graphene/Cu substrate by *vacuum deposition* and then the hydrogenation was carried out at 1 atm of gaseous H_2 and under liquid N_2 [31]. Before the experiment, the stabilization of hydrogenated Fe nanoparticles on this support was predicted by DFT calculations, meanwhile the existence of Fe hydride is considered as nonreachable. Hydrogen was found to be released from hydrogenated Fe nanoparticles. In addition, a *thermal reduction* method was used for the synthesis of $Fe/Fe_3O_4/G$ nanocomposite electrode material, using iron oxalate and exfoliated graphene oxide as precursors [32]. Its application, along with nickel, for rechargeable Ni/Fe

alkaline batteries (discharge and charge capacities of 280 mAh/g) in hybrid electric vehicles can be applied in a large-scale production.

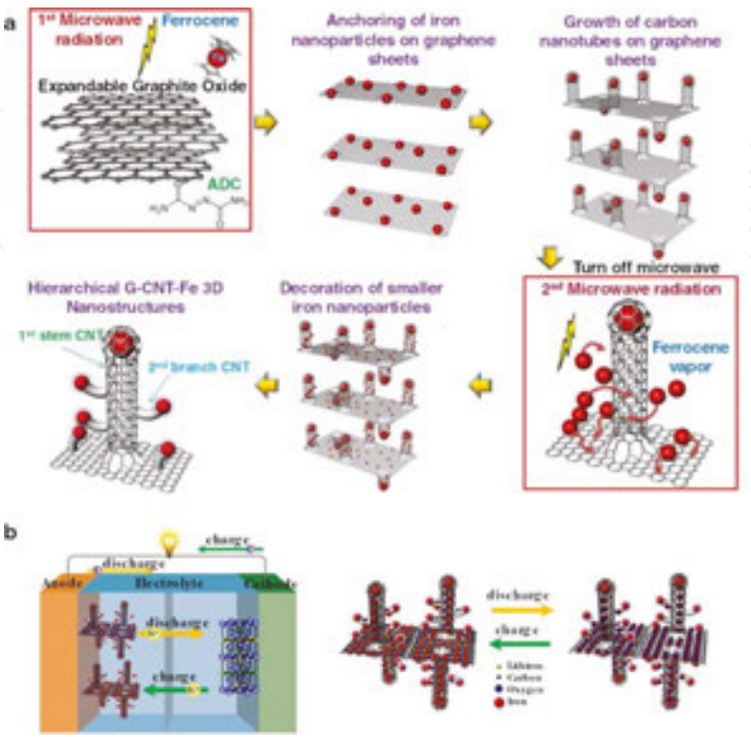

Figure 7. Two-step synthesis of hierarchical G-CNT-Fe 3D nanostructure and its application to anode material in lithium-ion batteries. (a) Step 1: microwave reaction for carbon nanotube growth. Step 2: iron nanoparticle decoration and fast explosive growth of smaller carbon nanotubes on original carbon nanotubes and graphene. (b) Schematic diagram for charge and discharge in G-CNT-Fe 3D anode material. Reproduced with permission from the *American Chemical Society*.

Sodium borohydride has been frequently used as classic reductive agent for the reduction of iron ions and/or GO. Thus, nano zero-valent iron (nZVI) -decorated graphene sheets were prepared via sodium borohydride reduction of GO and applied for Cr(VI) removal [33]. In a related report [34], nonhazardous superparamagnetic nanocomposites, consisting of iron nanoparticles (5 nm) and graphene, were synthesized from GO through intermediate formation of Fe^{3+}/GO complexes and their further reduction with $NaBH_4$. Methyl blue solution, a dye often present in wastewater of dyeing industry, can easily be decolorized using this nanocomposite.

Iron/G (or GO), as well as iron oxide/G (or GO) hybrids, can also have applications in the catalysis area. A novel type of oxygen reduction reaction (ORR) electrocatalyst on the basis of few-walled (2–3 walls) CNT-G complexes was reported [35]. Abundant defects on the outer walls of the CNTs can be produced via partial unzipping of the outer CNTs walls and the formation of large quantities of graphene sheets, connected with the intact inner walls of the CNTs. These graphene sheets make easier the formation of catalytic sites for ORR on annealing in NH_3. Nitrogen doping and Fe impurities are responsible for higher ORR activity in the CNT-G complexes. It was established that Fe atoms are often close to N atoms and are frequently

http://dx.doi.org/10.5772/64319

situated along edges of defective graphene sheets. Elimination of Fe by purification leads to a considerable decrease in ORR activity. Indeed, both nitrogen and iron atomic species are important to the high ORR electrocatalytic activity. Another example is a cost-effective synthesis of nitrogen-doped graphene (NG; **Figure 8**) carried out by using cyanamide as a nitrogen source and graphene oxide as a precursor; iron nanoparticles were incorporated into NG using $FeCl_3$ as precursor [36]. This composite was used as a model for the elucidation of the influence of nonnoble metals on the electrocatalytic performance. The NG supported with iron nanoparticles (5 wt%) showed high current density (8.20 mA cm^2) in an alkaline solution and an excellent methanol crossover effect, high stability in distinct media, high surface area, among other advantages, in comparison with Pt and NG-based catalysts, thus allowing platinum replacement.

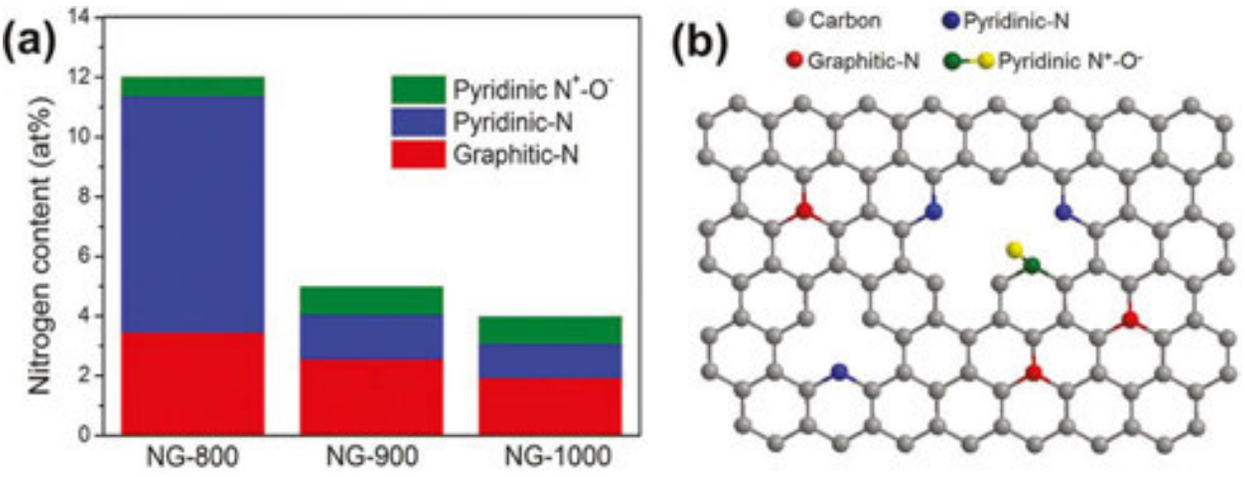

Figure 8. (a) The content of three types of nitrogen in NG. (b) Schematic representation of NG. Reproduced with permission from the *American Chemical Society*.

Environmental problems of contamination with heavy metals and other pollutants (As, Cr) can be partially solved using iron/graphene composites, in particular those containing iron in both metallic and oxidized form. A one-pot thermal decomposition method was used for the preparation of graphene nanoplatelet composites decorated with core-shell Fe-Fe_2O_3 nanoparticles [37]. These nanocomposites could be separated from the liquid-phase mixture with the aid of a permanent magnet. Efficient and effective adsorption of arsenic(III) from the polluted water was observed for this material (nearly complete As(III) removal within 1 ppb) and attributed to the increased adsorption sites existing in the presence of magnetic nanoparticles. Magnetic graphene nanocomposites (MGNCs), consisting of a core@double-shell structure of the nanoparticles with crystalline Fe as the core, iron oxide as the inner shell, and amorphous Si-S-O compound as the outer shell, were prepared by a thermodecomposition process (**Figure 9**) [38]. These composites were highly stable even in 1 M HCl aqueous acid and showed a fast and highly efficient removal of Cr(VI) from wastewater after 5 min (**Figure 10**), in contrast to several other materials (like carbon or waste biomass), the use of which require several hours or days and are not able to achieve 100% removal of Cr(VI).

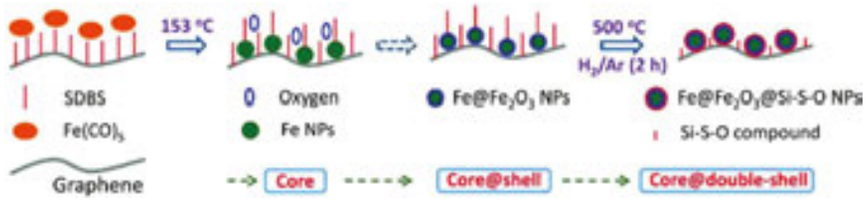

Figure 9. Schematic illustration of the formation of the MGNCs. Reproduced with permission from the *American Chemical Society*.

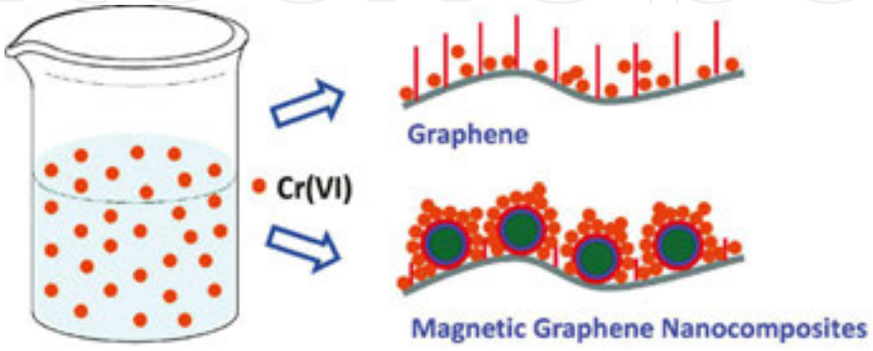

Figure 10. Schematic adsorption mechanisms on graphene and MGNCs. Reproduced with permission from the *American Chemical Society*.

Another application is related to polymers: graphene nanosheets, consisting of iron core and iron oxide shell nanoparticles, G/Fe@Fe_2O_3, were used as nanofillers for the fabrication of magnetic epoxy resin polymer nanocomposites [39]. The G/Fe@Fe_2O_3 was found to favor char formation from the epoxy resin; in addition, the tensile strength of polymer nanocomposite with 1.0 wt% Gr/Fe@Fe_2O_3 was found to be 58% higher than that of the pure epoxy and it was attributed to the high stiffness of graphene. It was suggested that the porous char layer with Gr/Fe@Fe_2O_3 may indicate the existence of Fe@Fe_2O_3, which helps the formation of gas, during the decomposition process of epoxy resin.

3. Fe_2O_3-graphene hybrids

Iron can be present in graphene composites in the elemental form (as shown above) or as Fe core/oxide shell nanoparticles, iron oxides, among others. The ratio of iron nanoforms in *different oxidation states* depends, in particular, on O-containing groups present in the graphene surface, use of reductants, and other conditions. Magnetic iron-containing nanoparticles were loaded on the GO sheets due to the abundant oxygen-containing functionalities present in these carbon materials (hydroxyl, epoxy, and carboxyl functional groups), and their growth mechanism was studied [40]. Most of these functional groups were eliminated and the magnetic nanoparticles were partially converted to iron during thermal treatment under reducing conditions. Metal nanoparticles changed the GO lattice structure and intrinsic functionalities; this effect depended on the amount of iron precursor.

http://dx.doi.org/10.5772/64319

The *effect of pH* is also very important and it was studied for several noncovalent magnetic GO-based materials, prepared using Fe_2O_3 microparticles, nanoparticles, and magnetic surfactants [41]. pH adjustment was used to effectively charge repulsion or attraction between Fe_2O_3 particles and the GO sheets (**Figure 11**). Each material caused coflocculation of GO at acidic pH, leading to materials that could be captured using an external magnetic field. The adsorption of GO at low pH was explained by attractive electrical double-layer forces between the GO and Fe_2O_3 or surfactants. On the contrary, at higher values of pH, the dispersions are stable due to alike-charge repulsions. An intriguing effect was found with Fe_2O_3 nanoparticles: low concentrations resulted in the flocculation of GO and higher concentrations caused restabilization, which are explained by an effective overcharging of the GO surfaces. These systems were found to remove a model nanomaterial, gold nanoparticles, from water.

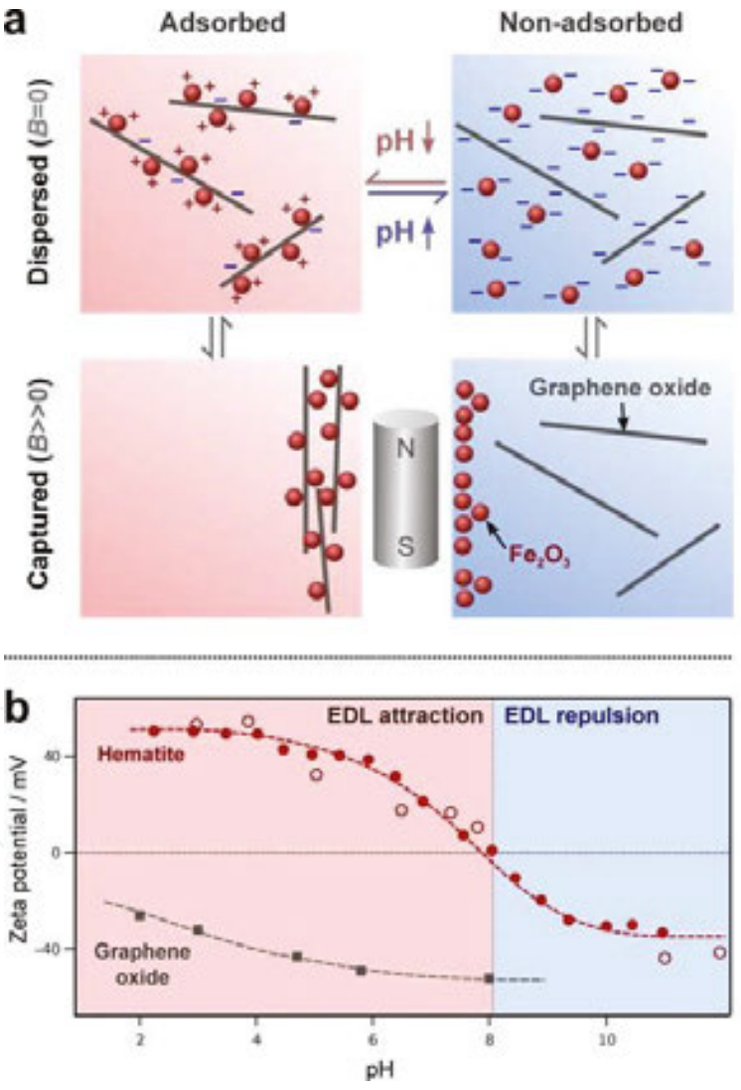

Figure 11. (a) Conceptual scheme of the experiment: pH adjustment is used to affect charge attraction or repulsion between the GO sheets and Fe_2O_3 particles. A magnetic field can be used to separate the Fe_2O_3 from solution or dispersion. (b) Zeta potentials of graphene oxide and Fe_2O_3, demonstrating the pH ranges at which electrical double-layer attraction or repulsion would be expected. Reproduced with permission from the *American Chemical Society*.

The main synthesis methods for iron(III) oxide/graphene nanohybrids are, in general, similar to those used for metals described above or Fe_3O_4 that are explained below. Thus, iron oxide nanoparticles encased by permeable carbon layers of few-layer graphene were synthesized by high-pressure pyrolysis of ferrocene with pristine graphene [42]. The ferrocene precursor provides both carbon and iron, leading to the carbon-coated iron oxide, while the graphene works as a high-surface-area anchor, to obtain small iron oxide nanoparticles. This material was used to improve the electrochemical performance of iron-oxide-based electrodes on Li-ion batteries. Similarly, an iron-oleate precursor (**Figure 12**) was used for the preparation of an iron-oxide/graphene nanocomposite via a solventless thermal decomposition method [43]. Highly monodisperse γ-Fe_2O_3 nanoparticles were found to be in close contact with graphene. This nanomaterial can serve as a potentially valuable candidate anode material for high-rate Li-ion batteries.

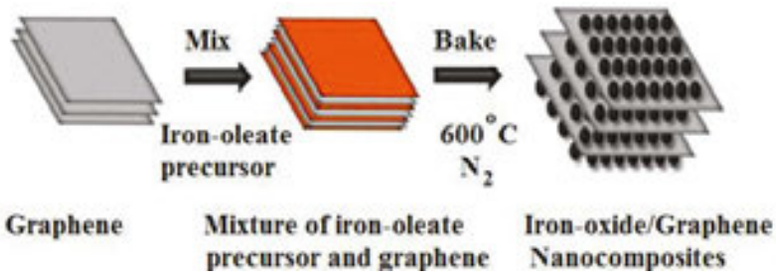

Figure 12. Schematic representation of the direct preparation of iron-oxide/graphene nanocomposites by the solventless thermal decomposition method. Reproduced with permission from the *Royal Society of Chemistry*.

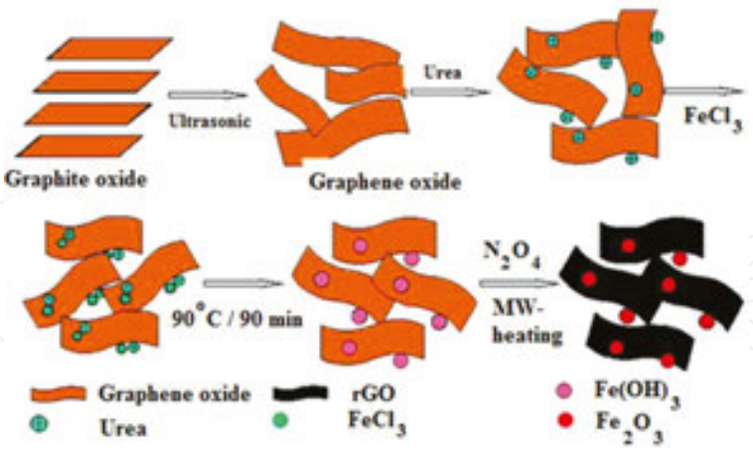

Figure 13. Scheme of the formation of the rGO/Fe_2O_3 composite. Reproduced with permission from the *American Chemical Society*.

In addition to high-temperature destructive methods, sol-gel and coprecipitation techniques are also common. Thus, reduced graphene oxide (rGO) tethered with maghemite (γ-Fe_2O_3) was prepared by a sol-gel process without a reducing agent in which sodium dodecylbenzenesulfonate (NaDDBS) was added into the suspension for the prevention of undesirable

http://dx.doi.org/10.5772/64319

formation of an iron oxide 3D network [44]. These composites were applied as anodes for half lithium-ion cells, exhibiting improved cycle life, reversible capacity, and good rate capability. Two-step synthesis (**Figure 13**), consisting of homogeneous precipitation and subsequent microwave-assisted reduction of the GO with hydrazine, led to reduced graphene oxide (rGO) platelets decorated with Fe_2O_3 nanoparticles, uniformly distributed on the surface of platelets [45]. The total specific capacity of rGO/Fe_2O_3 was determined to be higher than the sum of pure rGO and nanoparticular Fe_2O_3. In addition, polypyrrole (PPy) was reinforced with rGO and Fe_2O_3 to reach electrochemical stability and enhancement [46]. This ternary nanocomposite film was fabricated using a one-pot chronoamperometry approach.

In addition to their use in batteries, as referred above, a few other uses are known for Fe_2O_3/G hybrids. Thus, functional nanocomposite-based selective separation of microcystin-LR (toxin belonging to the family of microcystins produced by cyanobacteria and known to be the most toxic of this group) from contaminated water was achieved (**Figure 14**), applying cyclodextrin-functionalized magnetic composites consisting in porous silica and colloidal graphene [47]. In this material, the magnetic component offers easier separation of microcystin-LR from water and the cyclodextrin constituent offers host-guest interaction with microcystin-LR. Among all experimented cyclodextrins, γ-cyclodextrin was found to offer the best performance. The studied functional nanomaterials can be used for the development of advanced water purification systems. Catalytic applications are also reported, for example, for nanosized Fe_2O_3 composites on carbon matrix, modified with nitrogen-doped graphene (**Figure 15**), that are excellent catalysts for the chemoselective hydrogenation of nitroarenes to anilines with good yields (reaction (8)) [48].

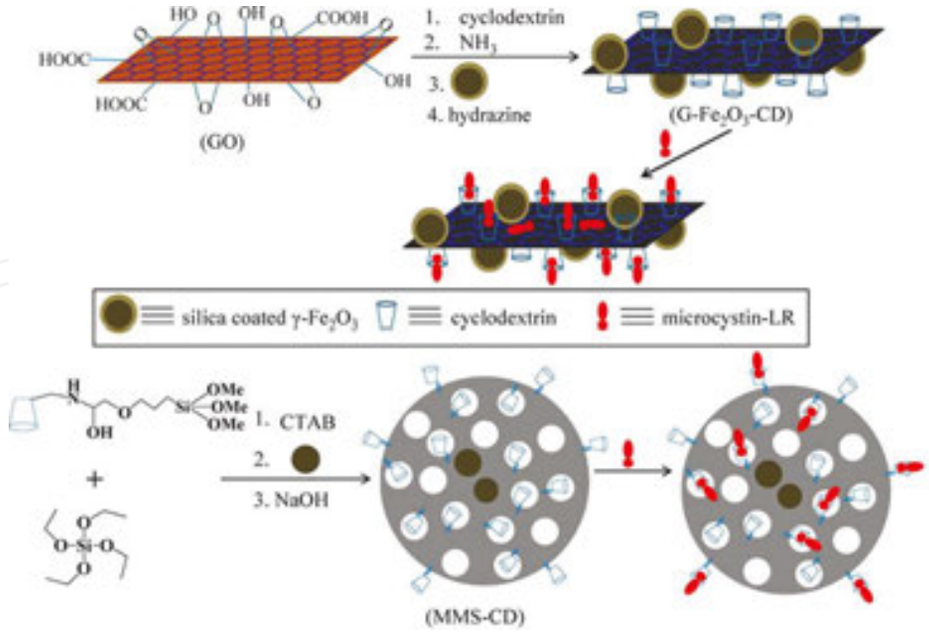

Figure 14. Synthesis strategies for cyclodextrin functionalized magnetic graphene composite (G-Fe_2O_3-CD) and cyclodextrin functionalized magnetic mesoporous silica (MMS-CD). Reproduced with permission from the *American Chemical Society*.

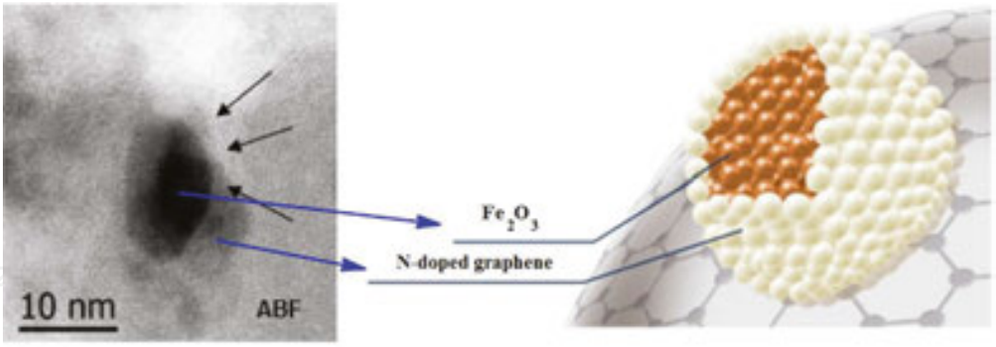

Figure 15. Nanoscaled Fe_2O_3 particles surrounded by N-doped graphene layers. Reproduced with permission from the *American Chemical Society*.

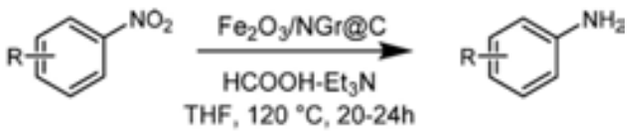

(8)

4. Fe_3O_4-graphene composites

4.1. Fe_3O_4/G aerogels

Among a large variety of mixed-valent-iron-oxide/graphene (or GO) composites, considerable attention is paid to *aerogels* in contrast to the above-described magnetic graphene hybrids. Graphene and other aerogels and routes for their synthesis are well known [49]. The introduction of a magnetic component could lead to a larger variety of unusual properties and potential applications, namely, the easy removal of pollutants, such as crude oil. These nanocomposites can have a simple composition (i.e., Fe_3O_4/G) or contain an additional component like a polymer. Thus, 3D N-doped graphene aerogel (N-GA)-supported Fe_3O_4 nanoparticles (Fe_3O_4/N-GAs; **Figure 16**) are known as efficient cathode catalysts for the oxygen reduction reaction (ORR) [50]. These hybrids were prepared via a combined hydrothermal self-assembly, freeze-drying, and thermal treatment process (**Figure 17**). The products showed an excellent electrocatalytic activity for the ORR in alkaline electrolytes, including a lower ring current, higher current density, higher electron transfer number (~4), lower H_2O_2 yield, and better durability.

3D graphene aerogels containing Fe_3O_4 nanoparticles (Fe_3O_4/GA (**Figure 18**), the lightest magnetic elastomer ever reported with density about 5.8 mg·cm^3) were hydrothermally prepared by self-assembly of graphene, simultaneously decorated with Fe_3O_4 nanoparticles [51]. They can be used to monitor the degree of compression/stretching of the material due to up to 52% reversible magnetic-field-induced strain and strain-dependent electrical resistance.

http://dx.doi.org/10.5772/64319

Among more complex aerogels, hydrophobic graphene aerogel/Fe_3O_4/polystyrene composites (having extremely low density of 0.005 g cm^{-3}, which corresponds to a volume porosity of 99.7%), with reticulated graphene structure, were solvothermally produced (**Figure 19**) [52]. Porous Fe_3O_4 nanoparticles were found to appear as partial substitutes for ethylenediamine-assisted cross-linking and interconnections between graphene plates. These composites were applied for crude oil remediation, allowing intake capacity as much as 40 times its own mass, after 10 water-oil separation cycles.

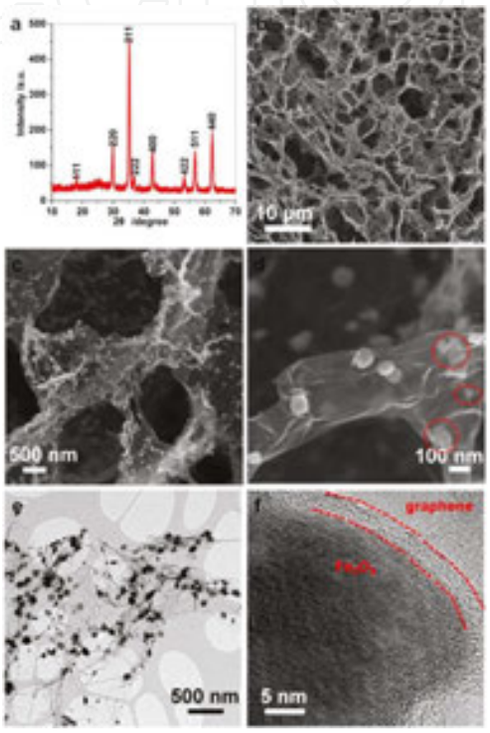

Figure 16. Structure and morphology of Fe_3O_4/N-GAs catalysts. (a) XRD pattern and (b–d) typical SEM images of Fe_3O_4/N-Gas, revealing the 3D macroporous structure and uniform distribution of Fe_3O_4 nanoparticles in the graphene aerogels. The red rings in (d) indicate Fe_3O_4 nanoparticles encapsulated in thin graphene layers. Representative (e) TEM and (f) HRTEM images of Fe_3O_4/N-GAs showing an Fe_3O_4 nanoparticle wrapped by graphene layers. Reproduced with permission from the *American Chemical Society*.

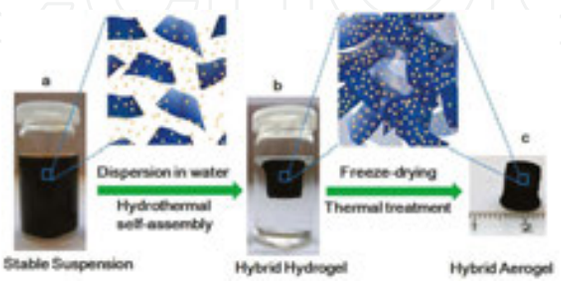

Figure 17. Fabrication process for the 3D Fe_3O_4/N-GAs catalyst. (a) Stable suspension of GO, iron ions, and polypyrrole (PPy) dispersed in a vial. (b) Fe- and PPy-supporting graphene hybrid hydrogel prepared by hydrothermal self-assembly and floating on water in a vial, and its ideal assembled model. (c) Monolithic Fe_3O_4/N-GAs hybrid aerogel obtained after freeze-drying and thermal treatment. Reproduced with permission from the *American Chemical Society*.

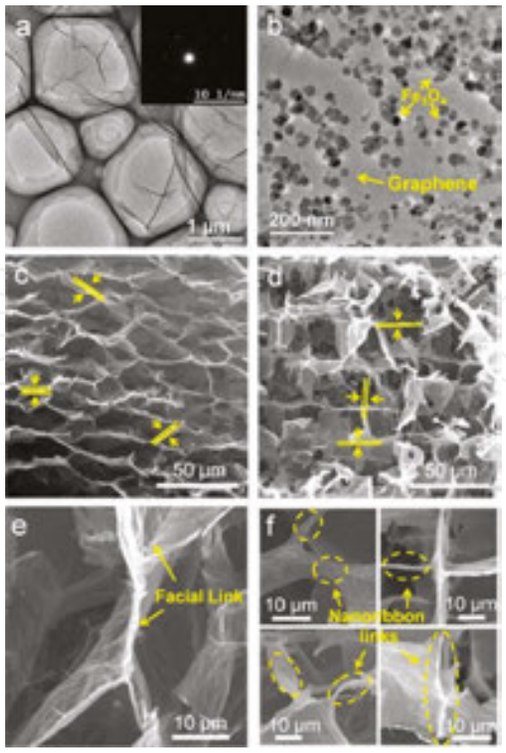

Figure 18. TEM and SEM images of the GA and Fe_3O_4/GA. (a) TEM image of GO and the diffraction pattern of a single flake (inset). (b) TEM image of Fe_3O_4 nanoparticle-decorated graphene sheets. (c, d) SEM images of microporous structures of GA and Fe_3O_4/GA. (e, f) SEM images of cross-linking patterns of GA and Fe_3O_4/GA. Reproduced with permission from the *American Chemical Society*.

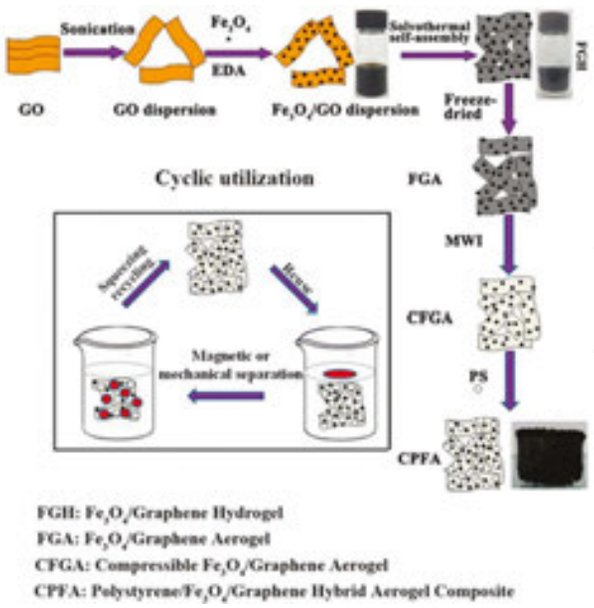

Figure 19. Schematic illustration of the fabrication process of the graphene aerogel/Fe_3O_4/polystyrene composites CPFA and its cyclic utilization for oil removal in water. Reproduced with permission from the *American Chemical Society*.

4.2. Bicomponent Fe_3O_4/G hybrids

Regarding the nonaerogel type of graphene-Fe_3O_4 hybrids, the hydrothermal [53] and solvothermal synthesis [54] have also been widely used although other methods are also frequently used, such as the atomic layer deposition, applied not only for Fe_3O_4/graphene but also for Ni/graphene composites [55]. Magnetic graphene foam with porous and hierarchical structures, on the basis of magnetite nanoparticles, was solvothermally obtained by gaseous reduction in a hydrothermal system and used for the adsorption of oil and organic solvents, thus serving for the cleanup of oil spills [56]. Fe_3O_4 nanoparticles on graphene foam possessed different morphologies, nanosheet arrays, or cubic structures, while controlling the reduction degree of graphene oxide under mild conditions. Distinct ratios "iron oxide/graphene" are important for several applications. Thus, G/Fe_3O_4 nanocomposites with different ratios of Fe_3O_4 to GO (mFe_3O_4: mG = 0.1:1, 0.2:1, 0.4:1, 0.6:1, 0.8:1 and 1:1) were prepared by solvothermal method and used for the removal of methylene blue dye from aqueous solutions [57]. The following morphologies were observed: uniform spherical homogeneously distributed Fe_3O_4 nanoparticles, with no agglomeration over the graphene sheets, and a uniform sheet-like shape of prepared graphene. Increasing the Fe_3O_4 nanoparticles on the surface of the graphene sheet was found to decrease the adsorption capacity, while the magnetization increased.

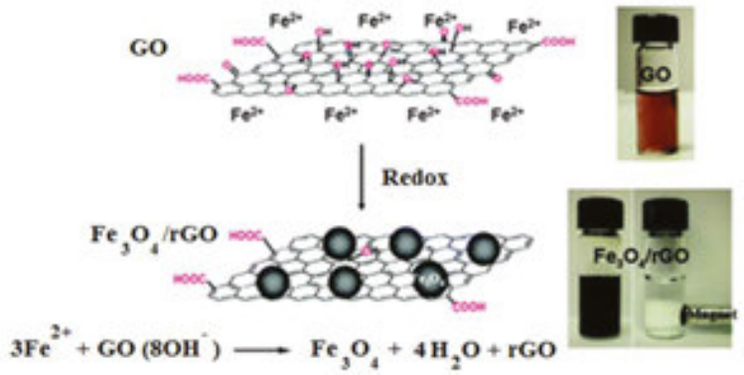

Figure 20. (a) A schematic representation of the preparation route of Fe_3O_4/rGO via a redox reaction between GO and Fe^{2+}. Photos show a water/NH_4OH (pH = 9) solution of Fe_3O_4/rGO (b) before and (c, left panel) after the redox reaction with Fe^{2+}, and (c, right panel) with an applied magnet. Reproduced with permission from the *Royal Society of Chemistry*.

Several methods, considered as "greener", are sometimes reported for iron oxide/graphene composites. Thus, the "green" oxidation of Fe^{2+} cations in $FeCl_2$ or $FeSO_4$ by graphene oxide led to an *in situ* deposition of Fe_3O_4 nanoparticles onto the self-reduced graphene oxide (rGO) sheets (**Figure 20**) [58]. Strongly supraparamagnetic with highly chemical reactivity, electrical conductivity, good solubility, and excellent processability G@Fe_3O_4 nanocomposites (with an average diameter of Fe_3O_4 nanoparticles of 1.2–6.3 nm; coverage density of Fe_3O_4 nanoparticles on graphene nanosheets of 5.3–57.9%) were prepared by a one-step "green" procedure (**Figure 21**) [59]. In addition, an approach for the deposition of iron oxide nanoparticles with *selective narrow size distribution* (0.5–7 and 1–3 μm), supported on different sizes of graphene oxide by coprecipitation, using Fe^{2+} and Fe^{3+} aqueous salt solutions and NH_3, is described in reaction (9) [60]. The reduction of mitochondrial activity using these

materials is size dependent, but the chemical functionalization of GO and Fe_3O_4 is a way to enhance the biocompatibility, making the system independent of the size distribution of GO.

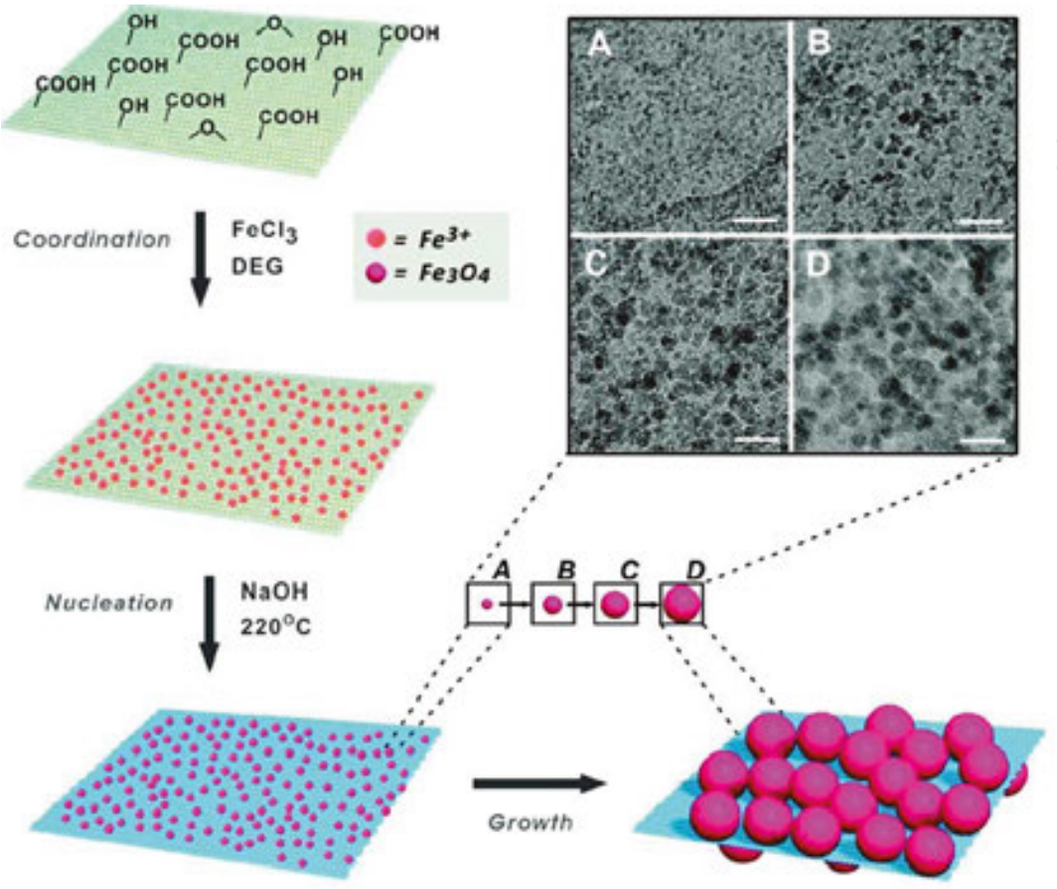

Figure 21. Schematic illustration of the formation of graphene@Fe_3O_4. The inset shows TEM images of graphene@Fe_3O_4 at reaction times of 0 (A), 1 (B), 5 (C), and 60 min (D). Scale bars are 20 nm. Reproduced with permission from the *American Chemical Society*.

$$(NH_4)_2Fe(SO_4)_2 \cdot 6H_2O + 2NH_4Fe(SO_4)_2 \cdot 12H_2O + 8NH_3 \cdot H_2O \rightarrow Fe_3O_4 \cdot 4H_2O + 6(NH_4)_2SO_4 + 14H_2O \quad (9)$$

4.3. Multicomponent Fe_3O_4/G hybrids

More complex Fe_3O_4/G- and organic(inorganic)-containing systems are also common. Thus, coating a layer of mesoporous *silica* materials on each side of magnetic graphene, in the conditions of CTAB-assisted sol-gel process, with further calcination, led to obtaining magnetic graphene double-sided mesoporous nanocomposites (G/SiO_2) with high surface area (168 cm^2/g) and large pore volume (0.2 cm^3/g) (**Figure 22**) [61]. The formed materials were applied to size-selective and specific enrichment and identification of peptides (peptidomics analysis) in human urine samples, protein digest solutions, and standard peptide mixtures. Another example is G@mSiO_2-C18 materials (with a surface area of 315 $cm^2 \cdot g^{-1}$ and a uniform pore size of 3.3 nm) with extended plate-like morphology, prepared by coating mesoporous silica layers

http://dx.doi.org/10.5772/64319

onto graphene via surfactant-mediated cocondensation sol-gel process, and applied as magnetic solid-phase adsorbents to the selective enrichment of phthalates in water [62].

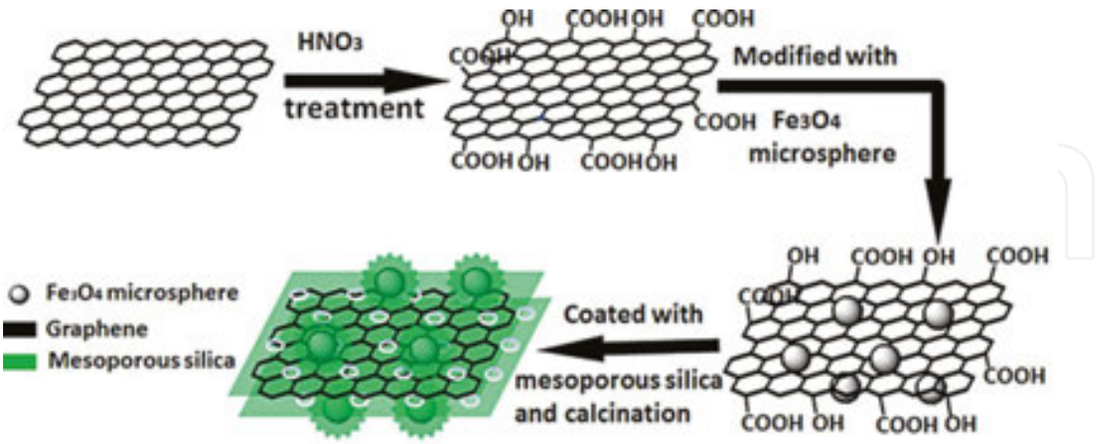

Figure 22. The workflow of synthesis of double-sided magnetic graphene/mSiO_2. Reproduced with permission from the *John Wiley & Sons*.

A few reports are dedicated to *chitosan-containing* magnetic materials with mainly biomedical applications. Thus, an iron oxide/graphene oxide/chitosan (Fe_3O_4/GO/CS) composite was obtained by a solution mixing-evaporation method [63]. Among other data, with the incorporation of 0.5 wt% Fe_3O_4 and 1 wt% GO, the tensile strength and Young's modulus of the composite significantly improved by about 28% and 74%, respectively, compared with chitosan. In addition, it was established from TGA that Fe_3O_4/GO/CS is less thermally stable than GO/CS composites, and graphite is more thermally stable than GO. In a related report [64], magnetic Fe_3O_4 nanoparticles were introduced into a water-dispersible and biocompatible chitosan-functionalized graphene, fabricated by a one-step ball milling of carboxylic chitosan and graphite. It could be an excellent catalyst for electrochemical biosensors, in particular for glucose detection, due to the presence of nitrogen (from chitosan) at the surface of graphene.

Also, superparamagnetic fluorescent Fe_3O_4/SiO_2/G-CdTe QD s/chitosan nanocomposites (Fe_3O_4/SiO_2/graphene-CdTe QDs/chitosan nanocomposites (FGQCs), with a spherical diameter of 467 nm; QDs: quantum dots) were prepared and studied for improving the drug loading content [65]. In addition, a magnetic composite bioadsorbent on the basis of magnetic chitosan and graphene oxide (MCGO) was prepared [66, 67]. Its adsorption capacity for methyl blue was found to be about 90% of the initial saturation adsorption capacity after being used four times. The adsorption of methyl blue on MCGO strongly depends on ionic strength and pH, showing an ion exchange mechanism.

In the case of *polymers*, integrated hybrid structures (stable for more than 1 year) consisting of exfoliated expanded graphite (EG flakes, both naked and functionalized with branched polyethylenimine (PEI)) and Fe_3O_4 nanocrystals were fabricated by an *ex situ* process by the integration of iron oxide nanoparticles, coated with meso-2,3-dimercaptosuccinic acid (DMSA) or poly(acrylic acid) (PAA), onto the exfoliated EG flakes under the support of *N*-hydroxysuccinnimide (NHS) and 1-ethyl-3-(3-dimethylaminopropyl)carbodiimide (EDC) [68]. Such

materials can have antibacterial properties. For example, *in situ* growth of silver nanoparticles onto the polyethylenimine (PEI)-mediated magnetic reduced GO resulted in a bactericidal material, Ag@rGO-Fe_3O_4-PEI composite (**Figure 23**) [69]. The material provides a very high killing rate of 99.9% for *E. coli* bacteria under a 0.5 min near-infrared (NIR) laser irradiation.

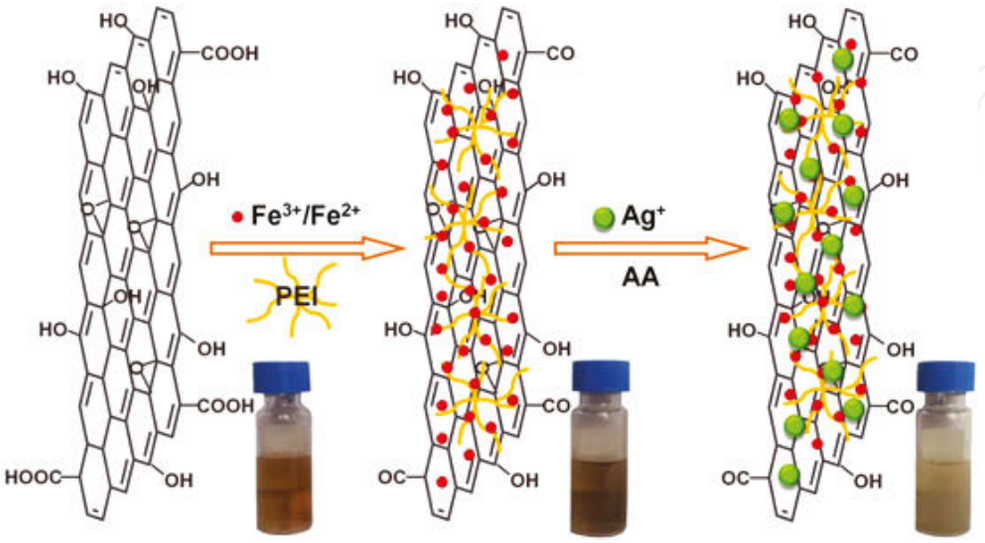

Figure 23. Schematic illustration of the preparation process of magnetic Ag@rGO-Fe_3O_4-PEI composites. Reproduced with permission from the *IOP Publishing*.

4.4. Applications of Fe_3O_4/G hybrids

Solvothermally prepared G/Fe_3O_4 (**Figure 24**) is able to effectively remove both bacteriophage and bacteria in water [70]. Indeed, it is capable of eliminating a wide range of pathogens including not only bacteriophages, but also various bacteria such as *Shigella*, *Salmonella*, *E. Faecium*, *E. coli*, *E. faecalis*, and *S. aureus*, with removal efficiencies up to 94%. Graphene oxide, particularly as magnetic Fe_3O_4/GO particles, was used as an adsorbent for wastewater treatment (**Figure 25**) [71]. A variety of other Fe_3O_4/G (or GO) hybrid applications are shown in **Table 1**.

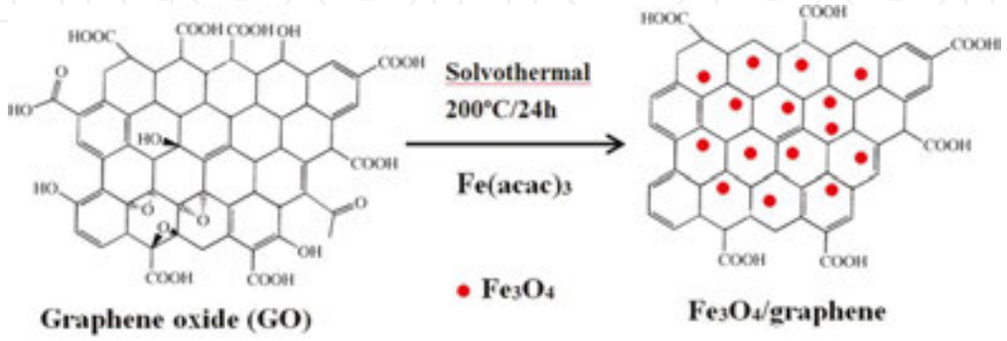

Figure 24. Synthesis route of G/Fe_3O_4. Reproduced with permission from the *American Chemical Society*.

http://dx.doi.org/10.5772/64319

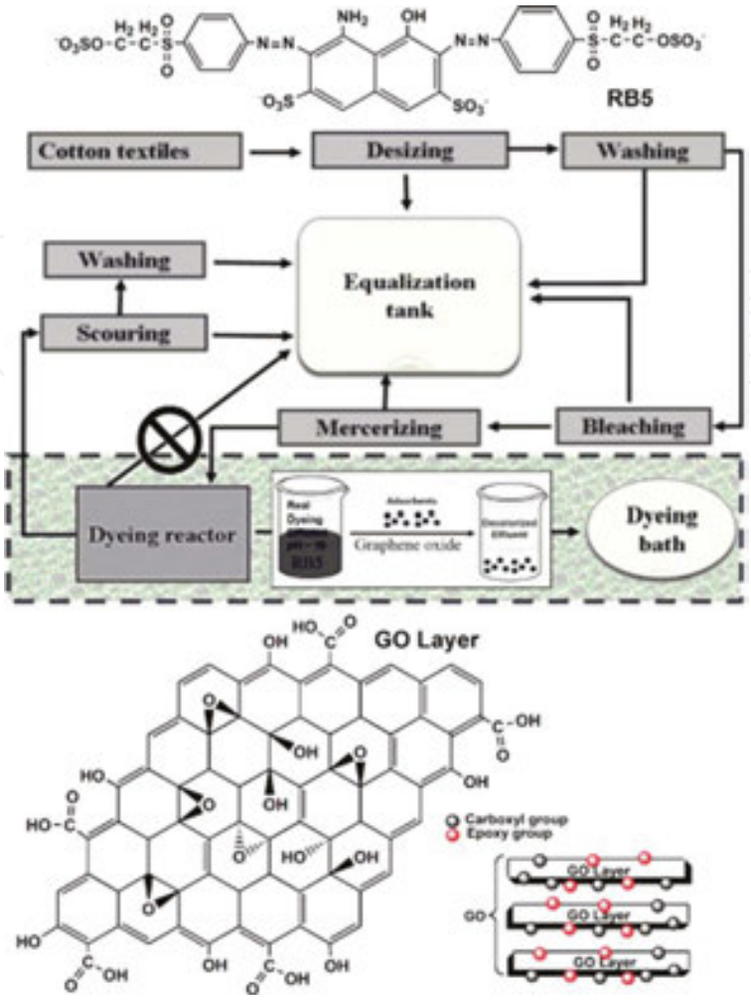

Figure 25. Illustrative scheme of the dyeing process and the proposed treatment of its effluents; RB5 dye (top) and functionalized GO adsorbent (bottom). Reproduced with permission from the *John Wiley & Sons*.

Composition	Description	Reference
Fe_3O_4/graphene aerogels	Removal of arsenic ions (up to 40.048 mg/g) from water	[72]
Fe_3O_4/graphene	Ultrahigh electrochemical sorption capacity for both inorganic arsenic species (arsenate As(V) and arsenite As(III)).	[73]
Magnetic graphene-oxide-supported-cyclodextrin	Heavy metal removal from wastewater. In particular, Cu(II) adsorption was found to be strongly pH-dependent and could be affected by background electrolytes, ionic strength, and citric acid.	[74]
Polyethylenimine(PEI)-modified magnetic mesoporous silica and graphene oxide (MMSP-GO)	These hierarchical composites are suitable for synergistic adsorptive simultaneous removal of heavy metal ions (Pb^{2+}, Cd^{2+}) and humic acid.	[75]
rGO/Fe_3O_4-based conductive and magnetic multifunctional films (membranes)	Can be produced and tested for its application in water desalination. Its potential uses also include catalysis, radiation shielding devices, biomedical fields, and supercapacitors.	[76]

Composition	Description	Reference
GO/Fe_3O_4	Super adsorbent to remove naphthalene, 1-naphthol, and 1-naphthylamine with different polarity. MWCNTs/FeO Fe_2O_3 were also produced in these synthesis as a byproduct, but graphene composite has the highest adsorption capacity among carbon-based nanomaterials. The adsorption capacity was shown to be naphthalene < 1-naphthol < 1-naphthylamine.	[77]
Magnetic graphene composite absorbent (Fe_3O_4@PDDA/GO@DNA) based on poly cationic core-shell Fe_3O_4@PDDA (poly(diallyldimethyl ammonium chloride) (PDDA)) and GO@DNA	Removal of trace levels of six types of polybrominated diphenyl ethers in water treatment. The nanomaterials can be reused at least 20 times for remediation purposes.	[78]
A porous graphene composite affinity material, containing graphene scaffolds, Fe_3O_4 nanoparticles, and fully covered porous titania nanostructures	Selective capture and convenient magnetic separation of target phosphopeptides, showing superior activity in comparison with commercial TiO_2 affinity materials.	[79]
3D graphene foam-supported Fe_3O_4	Use in lithium battery anodes.	[80]
The Fe_3O_4/G (graphene sheets) composite disks of μm dimensions	High-capacity lithium-ion battery anodes. The composites were prepared by electrostatic self-assembly between positively charged Fe_3O_4-APTMS [Fe_3O_4 grafted with (3-aminopropyl)trimethoxysilane (APTMS)] and negatively charged GO sheets and in an acidic solution (pH = 2) followed by *in situ* chemical reduction. An excellent rate capability as well as much enhanced cycling stability.	[81]

Table 1. Main applications of Fe_3O_4/G composites.

5. Ferrite-graphene and related composites

Simple or complex graphene or GO composites are known for a few ferrites, mainly those of cobalt and nickel, and usually used for environmental purposes or in batteries. $NiFe_2O_4$/G nanocomposites were prepared by mixing graphene and $NiFe_2O_4$ nanoparticles (obtained via a polyacrylamide gel method) into ethanol and further thermal drying at 60°C [82]. This composite exhibited significantly enhanced photocatalytic activity for the degradation of methylene blue in the conditions of irradiation of simulated sunlight, while $NiFe_2O_4$ nanoparticles were inert. NOH radicals were suggested as being the most active species causing dye degradation. $NiFe_2O_4$/GO nanohybrids based on $NiFe_2O_4$ and reduced GO consisted in nanosized $NiFe_2O_4$ crystals (5–10 nm in size) confined by few-layered rGO sheets [83]. This material seems a promising anode constituent for Li-ion batteries. The ternary nitrogen-doped graphene/nickel ferrite/polyaniline nanocomposite was hydrothermally prepared by a two-step approach process using urea, GO, $Ni(NO_3)_2 \cdot 6H_2O$, $Fe(NO_3)_3 \cdot 9H_2O$, and PANI as precur-

http://dx.doi.org/10.5772/64319

sors, and applied in electrodes for supercapacitors [84]. It was confirmed that the introduction of N-heteroatom greatly improved the electrode specific capacitance.

In the case of cobalt, its graphene composites have been synthesized mainly by hydro/solvothermally although an ultrasonic method was also reported [85]. A $CoFe_2O_4$/G nanocomposite was hydrothermally prepared and was evaluated in the photocatalytic degradation of methylene blue dye under visible irradiation [86]. Its photocatalytic activity depends on the surface area and the structural and optical properties of samples, and behaves better than pure cobalt ferrite. The formation mechanism of hydrothermally synthesized $CoFe_2O_4$-FGS (FGS: functionalized graphene sheets) is described in detail by Li et al. [87]. In addition, porous $CoFe_2O_4$/rGO nanoclusters with different concentrations of graphene were solvothermally prepared (**Figure 26**) [88] and their electrochemical properties were evaluated using polyvinylidene fluoride and Na-alginate as binder materials to improve the anode performance of Li-ion batteries. The resulting $CoFe_2O_4$/rGO (20%) nanocomposites with sodium alginate binders exhibited promising electrochemical performance, such as excellent recycling behavior, good rate capability, and high reversible capacity.

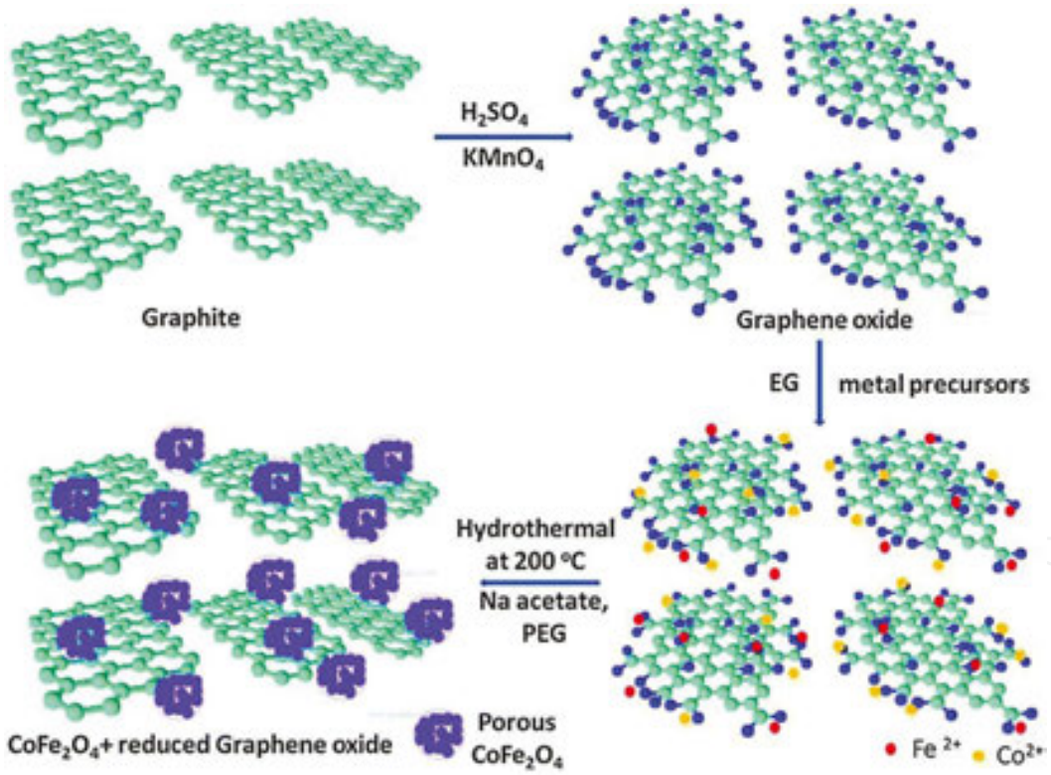

Figure 26. Synthesis of the $CoFe_2O_4$/rGO composite. Reproduced with permission from the *Royal Society of Chemistry*.

Other graphene- (or GO)-ferrite hybrids are rare (for example, zinc-ferrite-reduced graphene oxide [89]), and their synthesis, properties, and applications are similar to those of nickel and cobalt. Thus, in a solvothermally fabricated uniform copper ferrite nanoparticle-attached graphene nanosheet ($CuFe_2O_4$/G), $CuFe_2O_4$ nanoparticles (with a diameter of about 100 nm)

were shown to be densely and compactly deposited on graphene nanosheets [90]. This nanomaterial exhibited properties of a high-performance supercapacitor material. A related hydrothermal route was used for the formation of $CuFe_2O_4$ nanoparticles into the GO sheets, and the obtained material, with GO content varying from 10 to 30 wt%, was used as stable and good reproducible enzyme-free glucose sensor [91]. $MnFe_2O_4$ nanoparticle (MFNP)-decorated GO nanocomposites (MGONCs) were prepared through a miniemulsion and solvent evaporation process [92]. The loading of magnetic nanocrystals depends on the ratio of GO/magnetic nanoparticles. In a related report [93], $MnFe_2O_4$ nanoparticles were deposited on GO by thermal decomposition of manganese(II) acetylacetonate and iron(III) acetylacetonate precursors in triethylene glycol. The resulting GO/$MnFe_2O_4$ nanohybrids showed imperceptible *in vivo* toxicity, negligible hemolytic activity, and very low cytotoxicity, being effective T2 contrast agents.

In addition, barium hexaferrite nanoparticles, fabricated [94] via the citrate sol-gel combustion method, in a reaction medium consisting of various forms of graphene nanosheets (such as reduced graphite oxide, expanded graphite oxide, and expanded graphite) were used to prepare nanocomposites as microwave absorbing material for radars [95]. Finally, $BiFeO_3$ nanoparticles that are important materials in photocatalysis [96] were prepared via a polyacrylamide gel route and transformed into a $BiFeO_3$/G nanocomposite, by mixing with graphene in ethanol and further thermal drying at 60°C [97]. Methyl orange (MO) was found to be efficiently degraded by this material under simulated sunlight irradiation. This photocatalytic performance can be mainly ascribed to the efficient transfer of photogenerated electrons from $BiFeO_3$ to graphene (**Figure 27**). A similar reduced graphene rGO/$BiFeO_3$ nanocomposite, prepared by self-assembly, was also reported [98].

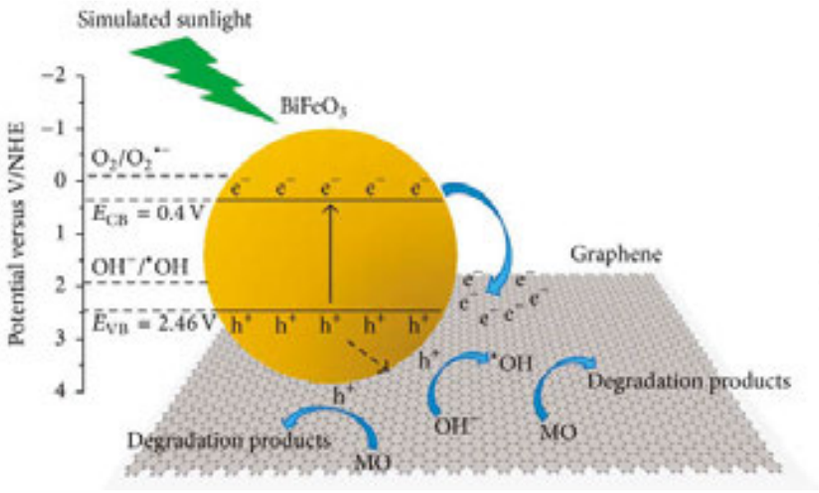

Figure 27. Schematic illustration of the photocatalytic mechanism of $BiFeO_3$-graphene nanocomposite toward the degradation of MO. Reproduced with permission from the *Hindawi Publishing Corporation.*

An interesting example of a magnetic molecule and its composite with graphene is known for lanthanides. A device made of a graphene nanoconstruction, decorated with $TbPc_2$ magnetic

http://dx.doi.org/10.5772/64319

molecules (Pc: phthalocyananine), was able to electrically detect the magnetization reversal of the molecules in proximity with graphene (**Figure 28**) [99, 100].

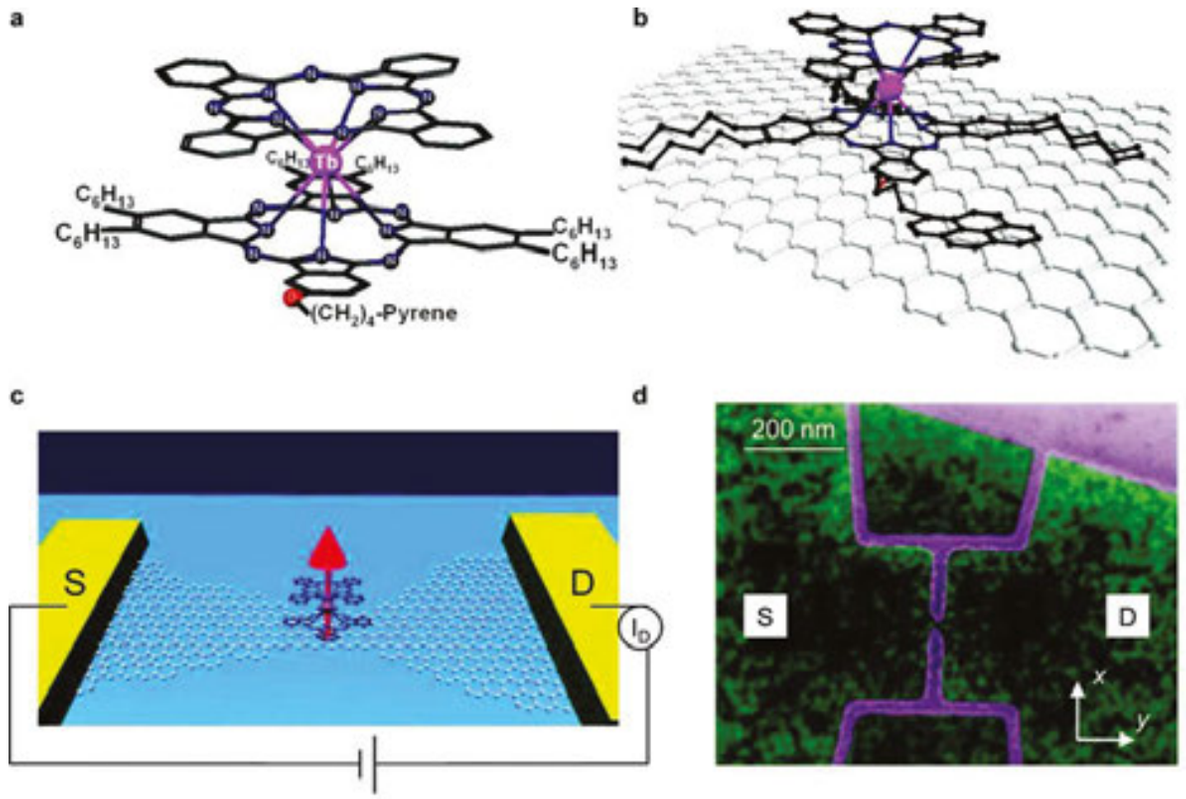

Figure 28. (a) Schematic representation of the $TbPc_2$ single-molecule magnet (SMM). (b, c) Schematic view of the device, showing in (b) the molecule attached to graphene and in (c) the nanoconstriction contacted by source (S) and drain (D) electrodes. The magnetic moments of the $TbPc_2$ SMMs (hexyl and pyrenyl groups here omitted for clarity) on top of the constriction add another degree of freedom to tune the conductivity of the device. (d) False-colored SEM image of the device presented in the text. SiO_2 substrate and etched graphene are colored in purple, while graphene conductive regions are colored in green. Source and drain electrodes are indicated. Reproduced with permission from the *American Chemical Society*.

6. Conclusions and outlook

The field of graphene and graphene oxide composites containing magnetic components can be considered as an important subject of the modern nanotechnology. Similarly to the filled or decorated carbon nanotubes, for which endohedral and exohedral functionalization with magnetic nanoparticles is well known, the graphene and graphene oxide magnetic nanocomposites can also be obtained via distinct methods and have a variety of applications. Graphene magnetic nanocomposites are currently known for those on the basis of elemental metals (Fe, Co, and Ni), magnetic nanoclusters, iron oxides (Fe_2O_3, Fe_3O_4) in distinct morphological forms, ferrites MFe_2O_4, 3D graphene aerogels@hierarchical Fe_3O_4 nanoclusters, single-molecule magnets such as $TbPc_2$ (Pc: phthalocyanine), other organometallic-containing composites

(benzene-metal-graphene), as well as polycomponent nanocomposites such as $Ag/Fe_3O_4/G$ (G: graphene), $Fe_3O_4/CdS/G$, or $FePc/Fe_3O_4/GO$ (GO :graphene oxide), etc.

Magnetic graphene and graphene oxide hybrids can be prepared by a variety of methods. Hydrothermal and solvothermal techniques are the most common. Other routes are also available, such as sol-gel autocombustion, sonoelectrochemical polymerization, thermal expansion and thermal reduction, microwave-assisted technique, as well as covalent bonding chemical methods. The formed composites have or might have several current and/or potential applications, such as devices (supercapacitors or material for anodes of lithium batteries), construction (graphene oxide-ferrofluid-cement nanocomposites), analytical, sensor, and biosensor applications (graphene-based magnetic solid-phase extraction for the determination of five chloroacetanilide herbicides (alachlor, acetochlor, metolachlor, butachlor, and pretilachlor), nitrite sensor, composites with peroxidase-like activity for colorimetric detection of glucose, etc.), environmental remediation (degradation and removal of water pollutants, such as chlorophenols, adsorbent for pesticide extraction, As and heavy metals (U^{VI})), compounds with antibacterial properties, and, of course, as magnetic nanocatalysts or nanophotocatalysts which can be simply magnetically removed from reaction media [101, 102].

As described above, magnetic graphene and graphene oxide composites can have applications, in particular, in the removal, decoloration, sequestration and adsorption of dyes [103], antibiotics and other organic contaminants, heavy metal separation (Hg, Cd, Cr, Cu, and As), and other environmental remediation aspects [104]. Other areas include biological imaging and further bioapplications [105], magnetic separation, electromagnetic materials and coatings, conducting polymer nanocomposites, aligned substrate for nanodevices, and spintronic devices with perpendicular magnetic anisotropy. 3D graphene aerogels can have applications in electrode materials, supercapacitors, oil absorption, and gas sensors due to their electrical conductivity, mechanical strength, and high porosity.

Author details

Oxana Vasilievna Kharissova[1], Beatriz Ortega García[1], Boris Ildusovich Kharisov[2*] and Ubaldo Ortiz Méndez[3]

*Address all correspondence to: bkhariss@hotmail.com

1 Department of Physico-Mathematics, Autonomous University of Nuevo León, Monterrey, Mexico

2 Department of Chemistry, Autonomous University of Nuevo León, Monterrey, Mexico

3 FIME (Department of Mechanical & Electrical Engineering), Autonomous University of Nuevo León, Monterrey, Mexico

References

[1] Liu, X.; Wang, C.-Z.; Hupalo, M.; Lin, H.-Q.; Ho, K.M.; Tringides, M.C. Metals on graphene: interactions, growth morphology, and thermal stability. Crystals, 2013, 3, 79–111.

[2] Lim, H.N.; Huang, N.M.; Chia, C.H.; Harrison, I.I. Inorganic nanostructures decorated graphene. In: Advanced Topics on Crystal Growth (Ed. Sukarno Olavo Ferreira), Intech, Rijeka, Croatia, 2013.

[3] Dahal, A.; Batzill, M. Graphene–nickel interfaces: a review. Nanoscale, 2014, 6, 2548–2562.

[4] Dhand, V.; Rhee, K.Y.; Kim, H.J.; Jung, D.H. A comprehensive review of graphene nanocomposites: research status and trends, J. Nanomater., 2013, 763953, 14 pp.

[5] Masotti, A.; Caporali, A. Preparation of magnetic carbon nanotubes (Mag-CNTs) for biomedical and biotechnological applications. Int. J. Mol. Sci., 2013, 14, 24619–24642.

[6] Hu, F.M.; Gubernatis, J.E.; Lin, H.-Q.; Li, Y.-C.; Nieminen, R.M. Behavior of a magnetic impurity in graphene in the presence of a vacancy. Phys. Rev. B, 2012, 85(11), 115442/1-5.

[7] Hu, F.M.; Ma, T.; Lin, H.-Q.; Gubernatis, J.E. Magnetic impurities in graphene. Phys. Rev. B, 2011, 84, 075414.

[8] Voloshina, E.; Dedkov, Yu. Electronic and magnetic properties of the graphene-ferromagnet interfaces: theory vs. experiment. In: Physics and Applications of Graphene—Experiments (Ed. Mikhailov, S.), Intech, Rijeka, Croatia, 2011.

[9] Le, H.M.; Hirao, H.; Kawazoe, Y.; Nguyen-Manh, D.J. Nanostructures of C_{60}-metal-graphene (metal = Ti, Cr, Mn, Fe, or Ni): a spin-polarized density functional theory study. Phys. Chem. C, 2014, 118, 21057−21065.

[10] Raji, A.T.; Lombardi, E.B. Stability, magnetic and electronic properties of cobalt–vacancy defect pairs in graphene: A first-principles study. Physica B, 2015, 464, 28–37.

[11] Li, B.; Xu, D.; Zhao, J.; Zeng, H. First principles study of electronic and magnetic properties of Co-doped armchair graphene nanoribbons. J. Nanomater., 2015, 538180, 9 pp.

[12] Donati, F.; Dubout, Q.; Autes, G.; Patthey, F.; Calleja, F.; Gambardella, P.; Yazyev, O.V.; Brune, H. Magnetic moment and anisotropy of individual Co atoms on graphene. Phys. Rev. Lett., 2013, 236801, 5 pp.

[13] Vita, H.; Bottcher, St.; Leicht, P.; Horn, K.; Shick, A.B.; Maca, F. Electronic structure and magnetic properties of cobalt intercalated in graphene on Ir(111). Phys. Rev. B, 2014, 90, 165432.

[14] Decker, R.; Brede, J.; Atodiresei, N.; Caciuc, V.; Blugel, S.; Wiesendanger, R. Atomic-scale magnetism of cobalt-intercalated graphene. Phys. Rev. B, 2013, 87, 041403(R).

[15] Rougemaille, N.; N'Diaye, A.T.; Coraux, J.; Vo-Van, C.; Fruchart, O.; Schmid, A.K. Perpendicular magnetic anisotropy of cobalt films intercalated under graphene. Appl. Phys. Lett., 2012, 101, 142403.

[16] Vermisoglou, E.C.; Devlin, E.; Giannakopoulou, T.; Romanos, G.; Boukos, N.; Psycharis, V.; Lei, C.; Lekakou, C.; Petridis, D.; Trapalis, C. Reduced graphene oxide/iron carbide nanocomposites for magnetic and supercapacitor applications. J. Alloys Compounds, 2014, 590, 102–109.

[17] Afshar, M.; Doosti, H. Magnetic properties of cobalt single layer added on graphene: a density functional theory study. Mod. Phys. Lett. B, 2015, 29(2), 1450262, 9 pp.

[18] Zhidkov, I.S.; Skorikov, N.A.; Korolev, A.V.; Kukharenko, A.I.; Kurmaev, E.Z.; Fedorov, V.E.; Cholakh, S.O. Electronic structure and magnetic properties of graphene/Co composites. Carbon, 2015, 91, 298–303.

[19] Lin, K.-Y.A.; Hsu, F.-K.; Lee, W.-D. Magnetic cobalt–graphene nanocomposite derived from self-assembly of MOFs with graphene oxide as an activator for peroxymonosulfate. J. Mater. Chem. A, 2015, 3, 9480–9490.

[20] Zhang, L.; Huang, Y.; Zhang, Y.; Ma, Y.; Chen, Y. Sol–gel autocombustion synthesis of graphene/cobalt magnetic nanocomposites. J. Nanosci. Nanotechnol., 2013, 13, 1129–1131.

[21] Yang, S.; Cui, G.; Pang, S.; Cao, Q.; Kolb, U.; Feng, X.; Maier, J.; Mullen, K. Fabrication of cobalt and cobalt oxide/graphene composites: towards high-performance anode materials for lithium ion batteries. ChemSusChem, 2010, 3, 236–239.

[22] Yao, Y.; Xu, C., Qin, J., Wei, F.; Rao, M.; Wang, S. Synthesis of magnetic cobalt nanoparticles anchored on graphene nanosheets and catalytic decomposition of Orange II. Ind. Eng. Chem. Res. 2013, 52, 17341−17350.

[23] Umair, A.; Raza, H. Controlled synthesis of bilayer graphene on nickel. Nanoscale Res. Lett., 2012, 7, 437.

[24] Dlubak, B.; Martin, M.-B.; Weatherup, R.S., Yang, H.; Deranlot, C.; Blume, R.; Schloegl, R.; Fert, A.; Anane, A.; Hofmann, S.; Seneor, P.; Robertson, J. Graphene-passivated nickel as an oxidation-resistant electrode for spintronics. ACS Nano, 2012, 6(12), 10930–10934.

[25] Sicot, M.; Bouvron, S.; Zander, O.; Rudiger, U.; Dedkov, Vu.S.; Fonin, M. Nucleation and growth of nickel nanoclusters on graphene Moire on Rh(111). Appl. Phys. Lett., 2010, 96, 093115.

[26] Mural, P.K.S.; Pawar, S.P.; Jayanthi, S.; Madras, G.; Sood, A.K.; Bose, S. Engineering nanostructures by decorating magnetic nanoparticles onto graphene oxide sheets to shield electromagnetic radiations. ACS Appl. Mater. Interf., 2015, 7, 16266−16278.

[27] Qu, W.; Zhang, L.; Chen, G. Magnetic loading of graphene–nickel nanoparticle hybrid for electrochemical sensing of carbohydrates. Biosens. Bioelectron., 2013, 42, 430–433.

[28] Fang, J.; Zha, W.; Kang, M.; Lu, S.; Cui, L.; Li, S. Microwave absorption response of nickel/graphene nanocomposites prepared by electrodeposition. J. Mater. Sci., 2013, 48, 8060–8067.

[29] Aravind, S.S.J.; Eswaraiah, V.; Ramaprabhu, S. Facile and simultaneous production of metal/metal oxide dispersed graphene nano composites by solar exfoliation. J. Mater. Chem. 2011, 21(43), 17094–17097.

[30] Lee, S.-H.; Sridhar, V.; Jung, J.-H.; Karthikeyan, K.; Lee, Y.S.; Mukherjee, R.; Koratkar, N.; Oh, I.-K. Graphene nanotube iron hierarchical nanostructure as lithium ion battery anode. ACS Nano, 2013, 785, 4242–4251.

[31] Takahashi, K.; Wang, Y.; Chiba, S.; Nakagawa, Y.; Isobe, S., Ohnuki, S. Low temperature hydrogenation of iron nanoparticles on graphene. Sci. Rep., 2014, 4, 4598.

[32] Kumar, H.; Shukla, A.K. Fabrication Fe/Fe_3O_4/graphene nanocomposite electrode material for rechargeable Ni/Fe batteries in hybrid electric vehicles. Int. Lett. Chem. Phys. Astron., 2013, 2013, 15–25.

[33] Jabeen, H.; Chandra, V., Jung, S.; Woo Lee, J.; Kim, K.S.; Bin Kim, S. Enhanced Cr(VI) removal using iron nanoparticle decorated graphene. Nanoscale, 2011, 3, 3583–3585.

[34] Guo, J.; Wang, R.; Weei Tjiu, W.; Pan, J.; Liu, T. Synthesis of Fe nanoparticles@graphene composites for environmental applications. J. Hazardous Mater., 2012, 225–226, 63–73.

[35] Li, Y.; Zhou, W.; Wang, H.; Xie, L.; Liang, Y.; Wei, F.; Idrobo, J.-C.; Pennycook, S.J.; Dai, H. An oxygen reduction electrocatalyst based on carbon nanotube–graphene complexes. Nat. Nanotechn., 2012, 7, 394–400.

[36] Parvez, K.; Yang, S., Hernandez, Y.; Winter, A.; Turchanin, A.; Feng, X.; Mullen, K. Nitrogen-doped graphene and its iron-based composite as efficient electrocatalysts for oxygen reduction reaction. ACS Nano, 2012, 6(11), 9541–9550.

[37] Zhu, J.; Sadu, R.; Wei, S.; Chen, D.H.; Haldolaarachchige, N.; Luo, Z.; Gomes, J.A.; Young, D.P.; Guo, Z. Magnetic graphene nanoplatelet composites toward arsenic removal. ECS J. Solid State Sci. Technol., 2012, 1(1), M1–M5.

[38] Zhu, J.; Wei, S.; Gu, H.; Rapole, S.B.; Wang, Q.; Luo, Z.; Haldolaarachchige, N.; Young, D.P.; Guo, Z. One-pot synthesis of magnetic graphene nanocomposites decorated with core@double-shell nanoparticles for fast chromium removal. Environ. Sci. Technol. 2012, 46, 977–985.

[39] Zhang, X.; Alloul, O.; He, Q.; Zhu, J.; Joseph Verde, M.; Li, Y.; Wei, S.; Guo, Z. Strengthened magnetic epoxy nanocomposites with protruding nanoparticles on the graphene nanosheets. Polymer, 2013, 54, 3594–3604.

[40] Wang, Y.; He, Q.; Qu, H.; Zhang, X.; Guo, J.; Zhu, J.; Zhao, G.; Colorado, H.A.; Yu, J. et al. Magnetic graphene oxide nanocomposites: nanoparticles growth mechanism and property analysis. J. Mater. Chem. C, 2014, 2, 9478–9488.

[41] McCoy, T.M.; Brown, P.; Eastoe, J.; Tabor, R.F. Noncovalent magnetic control and reversible recovery of graphene oxide using iron oxide and magnetic surfactants. ACS Appl. Mater. Interf., 2015, 7, 2124−2133.

[42] Sun, Z.; Madej, E.; Wiktor, C. et al. One-pot synthesis of carbon-coated nanostructured iron oxide on few-layer graphene for lithium-ion batteries. Chem. Eur. J., 2015, 21, 16154–16161.

[43] Jang, B.; B. Chae, O.; Park, S.-K.; Ha, J.; Oh, S.-M.; Na, H.B.; Piao, Y. Solventless synthesis of an iron-oxide/graphene nanocomposite and its application as an anode in high-rate Li-ion batteries. J. Mater. Chem. A, 2013, 1, 15442–15446.

[44] Tae Kim, I.; Magasinski, A.; Jacob, K.; Yushin, G.; Tannenbaum, R. Synthesis and electrochemical performance of reduced graphene oxide/maghemite composite anode for lithium ion batteries. Carbon, 2013, 52, 56–64.

[45] Zhu, X.; Zhu, Y.; Murali, S.; Stoller, M.D.; Ruoff, R.S. Nanostructured reduced graphene oxide/Fe_2O_3 composite as a high-performance anode material for lithium ion batteries. ACS Nano, 2011, 5(4), 3333–3338.

[46] Eeu, Y.C.; Lim, H.N.; Lim, Y.S.; Zakarya, S.A.; Huang, N.M. Electrodeposition of polypyrrole/reduced graphene oxide/iron oxide nanocomposite as supercapacitor electrode material. J. Nanomater., 2013, 2013, 653890, 6 pp.

[47] Sinh, A.; Jan, N.R. Separation of microcystin-LR by cyclodextrin-functionalized magnetic composite of colloidal graphene and porous silica. ACS Appl. Mater. Interf., 2015, 7, 9911–9919.

[48] Jagadeesh, R.V.; Natte, K.; Junge, H.; Beller, M. Nitrogen-doped graphene-activated iron-oxide-based nanocatalysts for selective transfer hydrogenation of nitroarenes. ACS Catal., 2015, 5, 1526−1529.

[49] Jung, S.M.; Jung, H.Y.; Dresselhaus, M.S.; Jung, J.J.; Kong, J. A facile route for 3D aerogels from nanostructured 1D and 2D materials. Sci. Rep., 2012, 2, 849.

[50] Wu, Z.-S.; Yang, S.; Sun, Y.; Parvez, K.; Feng, X.; Mu®llen, K. 3D nitrogen-doped graphene aerogel-supported Fe_3O_4 nanoparticles as efficient electrocatalysts for the oxygen reduction reaction. J. Am. Chem. Soc., 2012, 134, 9082−9085.

[51] Xu, X.; Li, H.; Zhang, Q.; Hu, H.; Zhao, Z.; Li, J.; Li, J.; Qiao, Yu.; Gogotsi, Yu. Self-sensing, ultralight, and conductive 3D graphene/iron oxide aerogel elastomer deformable in a magnetic field. ACS Nano, 2015, 9(4), 3969–3977.

[52] Zhou, S.; Jiang, W.; Wang, T.; Lu, Y. Highly hydrophobic, compressible, and magnetic polystyrene/Fe_3O_4/graphene aerogel composite for oil−water separation. Ind. Eng. Chem. Res., 2015, 54, 5460−5467.

[53] Ren, L.; Huang, S.; Fan, W.; Liu, T. One-step preparation of hierarchical superparamagnetic iron oxide/graphene composites via hydrothermal method. Appl. Surf. Sci., 2011, 258, 1132–1138.

[54] Fu, C.; Zhao, G.; Zhang, H.; Li, S. A facile route to controllable synthesis of Fe_3O_4/graphene composites and their application in lithium-ion batteries. Int. J. Electrochem. Sci., 2014, 9, 46–60.

[55] Wang, G.; Gao, Z.; Wan, G.; Lin, S.; Yang, P.; Qin, Y. Supported high-density magnetic nanoparticles on graphene by atomic layer deposition used as efficient synergistic microwave absorbers. Nanoresearch, 2014, 7(5), 704–716.

[56] Yang, S.; Chen, L.; Mu, L.; Ma, P.C. Magnetic graphene foam for efficient adsorption of oil and organic solvents. J. Colloid Interf. Sci., 2014, 430, 337–344.

[57] Farghali, M.A.; Salah El-Din, T.A.; Al-Enizi, A.M.; El Bahnasawy, R.M. Graphene/magnetite nanocomposite for potential environmental application. Int. J. Electrochem. Sci., 2015, 10, 529–537.

[58] Xue, Y.; Chen, H.; Yu, D. et al. Oxidizing metal ions with graphene oxide: the in situ formation of magnetic nanoparticles on self-reduced graphene sheets for multifunctional applications. Chem. Commun., 2011, 47, 11689–11691.

[59] He, H.; Gao, C. Supraparamagnetic, conductive, and processable multifunctional graphene nanosheets coated with high-density Fe_3O_4 nanoparticles. Appl. Mater. Interf., 2010, 2(11), 3201–3210.

[60] Urbas, K.; Aleksandrzak, M.; Jedrzejczak, M.; Jedrzejczak, M.; Rakoczy, R.; Chen, X.; Mijowska, E. Chemical and magnetic functionalization of graphene oxide as a route to enhance its biocompatibility. Nanoscale Res. Lett., 2014, 9, 656.

[61] Yin, P.; Sun, N.; Deng, C.; Li, Y.; Zhang, X.; Yang, P. Facile preparation of magnetic graphene double-sided mesoporous composites for the selective enrichment and analysis of endogenous peptides. Proteomics, 2013, 13, 2243–2250.

[62] Huang, D.; Wang, X.; Deng, C.; Song, G.; Cheng, H.; Zhang, X. Facile preparation of raisin-bread sandwich-structured magneticgraphene/mesoporous silica composites with C18-modified pore-walls for efficient enrichment of phthalates in environmental water. J. Chromatogr. A, 2014, 1325, 65–71.

[63] Yadav, M.; Rhee, K.Y.; Park, J.S.; Hui, D. Mechanical properties of Fe_3O_4/GO/chitosan composites. Composites: Part B, 2014, 66, 89–96.

[64] Zhang, W.; Li, X.; Zou, R.; Wu, H.; Shi, H.; Yu, S.; Liu, Y. Multifunctional glucose biosensors from Fe_3O_4 nanoparticles modified chitosan/graphene nanocomposites. Sci. Rep., 2015, 5, 11129.

[65] Ou, Y.; Wang, F.; Huang, Y.; Li, D.; Jiang, Y.; Qin, Q.-H.; Stachurski, Z.H.; Tricoli, A.; Zhang, T. Fabrication and cyto-compatibility of Fe_3O_4/SiO_2/graphene–CdTeQDs/CS nanocomposites for drug delivery. Colloids Surf. B: Biointerf., 2014, 117, 466–472.

[66] Fan, L.; Luo, C.; Li, X.; Lu, F.; Qiu, H.; Sun, M. Fabrication of novel magnetic chitosan grafted with graphene oxide to enhance adsorption properties for methyl blue. J. Hazardous Mater., 2012, 215–216, 272–279.

[67] Fan, L.; Luo, C.; Sun, M.; Li, X.; Lu, F.; Qiu, H. Preparation of novel magnetic chitosan/graphene oxide composite as effective adsorbents toward methylene blue. Bioresource Technol., 2012, 114, 703–706.

[68] Jovici, N.; Calatayud, M.P.; Sanz, B.; Montone, A.; Goya, G.F. Ex situ integration of iron oxide nanoparticles onto exfoliated expanded graphite flakes in aqueous suspension. J. Serb. Chem. Soc., 2014, 79(9), 1155–1167.

[69] Wang, N.; Hu, B.; Chen, M.-L.; Wang, J.-H. Polyethylenimine mediated silver nanoparticle-decorated magnetic graphene as a promising photothermal antibacterial agent. Nanotechnology, 2015, 26, 195703, 8 pp.

[70] Zhan, S.; Zhu, D.; Ma, S.; Yu, W.; Jia, Y.; Li, Y.; Yu, H.; Shen, Z. Highly efficient removal of pathogenic bacteria with magnetic graphene composite. ACS Appl. Mater. Interf., 2015, 7, 4290−4298.

[71] Kyzas, G.Z.; Deliyanni, E.A.; Matis, K.A. Graphene oxide and its application as an adsorbent for wastewater treatment. J. Chem. Technol. Biotechnol., 2014, 89, 196–205.

[72] Ye, Y.; Yin, D.; Wang, B.; Zhang, Q. Synthesis of three-dimensional Fe_3O_4/graphene aerogels for the removal of arsenic ions from water. J. Nanomater., 2015, 864864, 6 pp.

[73] Mishra, A.K.; Ramaprabhu, S. Ultrahigh arsenic sorption using iron oxide-graphene nanocomposite supercapacitor assembly. J. Appl. Phys., 2012, 112, 104315.

[74] Hu, X.-j.; Liu, Y.-g.; Wang, H.; Zeng, G.-m.; Hua, X.; Guo, Y.-m.; Li, T.-t.; Chen, A.-w.; Jiang, L.-h.; Guo, F.-y. Adsorption of copper by magnetic grapheneoxide-supported -cyclodextrin: Effects of pH, ionicstrength, background electrolytes, and citric acid. Chem. Chem. Eng. Res. Design, 2015, 93, 675–683.

[75] Wang, Y.; Liang, S.; Chen, B.; Guo, F.; Yu, S.; Tang, Y. Synergistic removal of Pb(II), Cd(II) and humic acid by Fe_3O_4@mesoporous silica-graphene oxide composites. PLOS ONE, 2013, 8(6), e65634.

[76] Narayanan, T.N.; Liu, Z.; Lakshmy, P.R.; Gao, W.; Nagaoka, Y.; Sakthi Kumar, D.; Lou, J.; Vajtai, R.; Ajayan, P.M. Synthesis of reduced graphene oxide–Fe_3O_4 multifunctional

freestanding membranes and their temperature dependent electronic transport properties. Carbon, 2012, 50, 1338–1345.

[77] Yang, X.; Li, J.; Wen, T.; Ren, X., Huang, Y.; Wang, X. Adsorption of naphthalene and its derivatives on magnetic graphene composites and the mechanism investigation. Colloids Surf. A: Physicochem. Eng. Aspects, 2013, 422, 118–125.

[78] Gan, N.; Zhang, J.; Lin, S.; Long, N.; Li, T.; Cao, Y. A novel magnetic graphene oxide composite absorbent for removing trace residues of polybrominated diphenyl ethers in water. Materials 2014, 7, 6028–6044.

[79] Cheng, G.; Yu, X.; Zhou, M.D.; Zheng, S.-Y. Preparation of magnetic graphene composites with hierarchical structure for selective capture of phosphopeptides. J. Mater. Chem. B, 2014, 2, 4711–4719.

[80] Luo, J.; Liu, J.; Zeng, Z. et al. Three-dimensional graphene foam supported Fe_3O_4 lithium battery anodes with long cycle life and high rate capability. Nano Lett., 2013, 13, 6136−6143.

[81] Yoon, T.; Kim, J.; Kim, J.; Kyoo Lee, J. Electrostatic self-assembly of Fe_3O_4 nanoparticles on graphene oxides for high capacity lithium-ion battery anodes. Energies, 2013, 6, 4830–4840.

[82] Zhao, D.F.; Yang, H., Li, R.S.; Ma, J.Y.; Feng, W.J. Fabrication of nickel ferrite–graphene nanocomposites and their photocatalytic properties. Mater. Res. Innovations, 2014, 18(7), 519–523.

[83] Zhu, P.; Liu, S.; Xie, J.; Zhang, S.; Cao, G.; Zhao, X. Facile synthesis of $NiFe_2O_4$/reduced graphene oxide hybrid with enhanced electrochemical lithium storage performance. J. Mater. Sci. Technol., 2014, 30(11), 1078–1083.

[84] Wang, W.; Hao, Q.; Lei, W.; Xia, X.; Wang, X. Ternary nitrogen-doped graphene/nickel ferrite/polyaniline nanocomposites for high-performance supercapacitors. J. Power Sources, 2014, 269, 250–259.

[85] Xiao, Y.; Li, X.; Zai, J.; Wang, K.; Gong, Y.; Li, B.; Han, Q.; Qian, X. $CoFe_2O_4$-graphene nanocomposites synthesized through an ultrasonic method with enhanced performances as anode materials for Li-ion batteries. Nano-Micro Lett., 2014, 6(4), 307–315.

[86] Suwanchawalit, C.; Somjit V. Hydrothermal synthesis of magnetic $CoFe_2O_4$-graphene nanocomposite with enhanced photocatalytic performance. Digest J. Nanomater. Biostruct, 2015, 10(3), 769–777.

[87] Li, N.; Zheng, M.; Chang, X.; Ji, G.; Lu, H.; Xue, L.; Pan, L.; Cao, J. Preparation of magnetic $CoFe_2O_4$-functionalized graphene sheets via a facile hydrothermal method and their adsorption properties. J. Solid State Chem., 2011, 184, 953–958.

[88] Ramesh Kumar, P.; Kollu, P.; Santhosh, C.; Eswara Varaprasada Rao, K.; Kim, D.K.; Nirmala Grace, A. Enhanced properties of porous $CoFe_2O_4$–reduced graphene oxide

composites with alginate binders for Li-ion battery applications. New J. Chem., 2014, 38, 3654–3661.

[89] Fei, P.; Zhong, M.; Lei, Z.; Su, B. One-pot solvothermal synthesized enhanced magnetic zinc ferrite–reduced graphene oxide composite material as adsorbent for methylene blue removal. Mater. Lett., 2013, 108, 72–74.

[90] Zhang, W.; Quan, B.; Lee, C.; et al. One-step facile solvothermal synthesis of copper ferrite−graphene composite as a high-performance supercapacitor material. ACS Appl. Mater. Interf., 2015, 7, 2404−2414.

[91] Shahnavaz, Z.; Woi, P.W.; Aliasn, Y. A hydrothermally prepared reduced graphene oxide-supported copper ferrite hybrid for glucose sensing. Ceram. Int., 2015, 41, 12710–12716.

[92] Peng, E.; Shi Guang Choo, E.; Chandrasekharan, P.; et al. Synthesis of manganese ferrite/graphene oxide nanocomposites for biomedical applications. Small, 2012, 8(23), 3620–3630.

[93] Yang, Y.; Shi, H.; Wang, Y.; et al. Graphene oxide/manganese ferrite nanohybrids for magnetic resonance imaging, photothermal therapy and drug delivery. J. Biomater. Appl. 2016 Jan;30(6):810–22. http://www.ncbi.nlm.nih.gov/pubmed/26296777

[94] Panwar, R.; Puthucheri, S.; Singh, D.; Agarwala, V. Design of ferrite–graphene-based thin broadband radar wave absorber for stealth application. IEEE Trans. Magnet., 2015, 51(1), 2802804, 4 pp.

[95] Durmus, Z.; Durmus, A.; Kavas, H. Synthesis and characterization of structural and magnetic properties of graphene/hard ferrite nanocomposites as microwave-absorbing material. J. Mater. Sci, 2015, 50, 1201–1213.

[96] Gao, T.; Chen, Z.; Huang, Q.; Niu, F.; Huang, X.; Qin, L.; Huang, Y. A review: preparation of bismuth ferrite nanoparticles and its applications in visible-light induced photocatalyses. Rev. Adv. Mater. Sci., 2015, 40, 97–109.

[97] Dai, J.F.; Xian, T.; Di, L.J.; Yang, H. Preparation of $BiFeO_3$-graphene nanocomposites and their enhanced photocatalytic activities. J. Nanomater., 2013, 642897, 5 pp.

[98] Li, T.; Shen, J.; Li, N.; Ye, M. Hydrothermal preparation, characterization and enhanced properties of reduced graphene-$BiFeO_3$ nanocomposite. Mater. Lett., 2013, 91, 42–44.

[99] Candini, A.; Klyatskaya, S.; Ruben, M.; Wernsdorfer, w.; Affronte, M. Graphene spintronic devices with molecular nanomagnets. Nano Lett., 2011, 11, 2634–2639.

[100] Lopes, M.; Candini, A.; Urdampilleta, M.; et al. Surface-enhanced Raman signal for terbium single-molecule magnets grafted on graphene. ACS Nano, 2010, 4(12), 7531–7537.

[101] Govan, J.; Gun'ko, Yu.K. Recent advances in the application of magnetic nanoparticles as a support for homogeneous catalysts. Nanomaterials, 2014, 4, 222–241.

[102] Lim, C.W.; Lee, I.S. Magnetically recyclable nanocatalyst systems for the organic reactions. Nano Today, 2010, 5, 412–434.

[103] Sivashankar, R.; Sathya, A.B.; Vasantharaj, K.; Sivasubramanian, V. Magnetic composite an environmental super adsorbent for dye sequestration—a review. Environ. Nanotechnol. Monit. Manage., 2014, 1–2, 36–49.

[104] Zhu, J.; Wei, S.; Chen, M.; Gu, H.; et al. Magnetic nanocomposites for environmental remediation. Adv. Powder Technol., 2013, 24, 459–467.

[105] Yin, P.T.; Shah, S.; Chhowalla, M.; Lee, K.-B. Design, Synthesis, and characterization of graphene–nanoparticle hybrid materials for bioapplications. Chem. Rev., 2015, 115(7), 2483–2531.

IntechOpen